Controls on knickpoint migration in a drainage network of the moderately uplifted Ardennes Plateau, Western Europe

Q1 A. Beckers,[1,2] B. Bovy,[1,3] E. Hallot[1] and A. Demoulin[1,4]*

[1] Dept of Physical Geography and Quaternary, University of Liege, Sart Tilman, B11, 4000 Liege, Belgium
[2] FRIA, 1000 Brussels, Belgium
[3] GIRPAS, Dept of Physics, University of Liege, Sart Tilman, B5, 4000 Liege, Belgium
[4] Fund for Scientific Research - FNRS, 1000 Brussels, Belgium

*Correspondence to: A. Demoulin, Dept of Physical Geography and Quaternary, University of Liege, Sart Tilman, B11, 4000 Liege, Belgium. E-mail: ademoulin@ulg.ac.be

ESPL
Earth Surface Processes and Landforms

ABSTRACT: Much research has been devoted to the development of numerical models of river incision. In settings where bedrock channel erosion prevails, numerous studies have used field data to calibrate the widely acknowledged stream power model of incision and to discuss the impact of variables that do not appear explicitly in the model's simplest form. However, most studies have been conducted in areas of active tectonics, displaying a clear geomorphic response to the tectonic signal. Here, we analyze the traces left in the drainage network 0.7 My after the Ardennes region (western Europe) underwent a moderate 100–150 m uplift. We identify a set of knickpoints that have traveled far upstream in the Ourthe catchment, following this tectonic perturbation. Using a misfit function based on time residuals, our best fit of the stream power model parameters yields $m = 0.75$ and $K = 4.63 \times 10^{-8}$ $m^{-0.5}y^{-1}$. Linear regression of the model time residuals against quantitative expressions of bedrock resistance to erosion shows that this variable does not correlate significantly with the residuals. By contrast, proxies for position in the drainage system prove to be able to explain 76% of the residual variance. High time residuals correlate with knickpoint position in small tributaries located in the downstream part of the Ourthe catchment, where some threshold was reached very early in the catchment's incision history. Removing the knickpoints stopped at such thresholds from the data set, we calculate an improved $m = 0.68$ and derive a scaling exponent of channel width against drainage area of 0.32, consistent with the average value compiled by Lague for steady state incising bedrock rivers. Copyright © 2014 John Wiley & Sons, Ltd.

KEYWORDS: fluvial incision; knickpoint migration; channel width; rock resistance control; erosion threshold; Ardennes

Introduction

Landscapes evolve as a product of the interplay between tectonics and climate, through the action of surface processes on more or less erodible substrates. Outside glaciated regions, landscape response to tectonic signals is determined by the way the drainage network reacts to the perturbation, with strong links between the nature of the response, its propagation speed over the entire catchment, and, consequently, the response time. The understanding of this transient adjustment relies heavily on the analysis of the fluvial incision mechanisms from reach to drainage network scales. In recent decades, theoretical studies have repeatedly shown that different erosion laws need to be used for alluvial and bedrock channel incision (Howard and Kerby, 1983; Willgoose *et al.*, 1991; Seidl and Dietrich, 1992; Sklar and Dietrich, 1998, 2004; Whipple and Tucker, 1999, 2002), and their implementation in numerical modeling highlighted specific behaviors of incising rivers (Crosby *et al.*, 2007). As the additional effects of non-tectonic variables such as rock type or rainfall amount are minimized by a high signal-to-noise ratio, most case studies concentrated so far on regions of strong incision, i.e. either high relief areas

submitted to high uplift rates (Crosby and Whipple, 2006; Wobus *et al.*, 2006; Berlin and Anderson, 2007; Yanites *et al.*, 2010) or small catchments where even a small base level change induces a clearly identifiable signal in the river profiles (Snyder *et al.*, 2000; Bishop *et al.*, 2005; Whittaker *et al.*, 2008). In such regions, these authors typically used detachment-limited models (where erosion rate is limited by the ability of the river to erode their channel bed) to best describe the physics of bedrock channel incision, and showed that the basic equation of the stream power class of models, which reduces erosion rate to a power function of drainage area and channel gradient, provides an approximate but potentially incomplete description of the observed erosion. While some of these studies concluded with recommendations for including explicitly additional variables such as channel width (Whittaker *et al.*, 2007a; Attal *et al.*, 2008; Yanites *et al.*, 2010), rainfall amount (Roe *et al.*, 2002) or uplift rate (Whittaker *et al.*, 2008) in the modeling, others emphasized the opposed tool and cover roles played by the river bed load transiting in bedrock channels. Bed load effects on erosion may be taken into account either by introducing a specific function in the classical stream power law (Whipple and Tucker, 2002; Turowski *et al.*, 2007; Cowie

et al., 2008) or by deriving a new erosion law directly from the characteristics of the flux of saltating bed load (Sklar and Dietrich, 2004, 2006). Recently, Lague *et al.* (2005) and Lague (2010) proposed a new model incorporating the temporally stochastic character of discharge and sediment supply.

Although often noting that local conditions deviated from typical knickpoint migration, e.g. in terms of erosion processes where the incision wave proceeds by waterfall recession (Hayakawa and Matsukura, 2009), many field studies of bedrock channel incision have made use of the presence of knickpoints in the long profiles of rivers in order to parameterize the stream power equation. Alternatively, they have adjusted the derived celerity equation, which expresses the migration rate of knickpoints across drainage networks, to known age and positions of a generation of retreating knickpoints. Such studies have generally shown that the stream power model yields a fairly good first-order representation of the drainage network response in actively uplifting areas (e.g. Bishop *et al.*, 2005; Anthony and Granger, 2007; Berlin and Anderson, 2007; Loget and Van Den Driessche, 2009; Cook *et al.*, 2009; Valla *et al.*, 2010; Zhang *et al.*, 2011; Jansen *et al.*, 2011; Castillo *et al.*, 2013). In agreement with the theory, most calculated values of the m/n ratio fall in the range 0.4–0.7 (m and n being the scaling exponents of erosion rate respectively with drainage area A and slope S in the stream power law).

However, this wealth of theoretical and field studies has also underlined several remaining research needs. For example, only recently have workers come to more detailed analyses of the interactions between incision and channel geometry, notably including lateral erosion and channel width variations (Stark, 2006; Lague, 2010, 2014). Observation of the role of channel aspect ratio in bedrock stream incision (Duvall *et al.*, 2004; Amos and Burbank, 2007; Whittaker *et al.*, 2007a, 2007b; Snyder and Kammer, 2008) clearly points to the transient alteration of the relation between channel width and drainage area (or discharge) in association with the passage of an erosion wave, confirming the recent findings of Whittaker *et al.* (2007a) and Attal *et al.* (2008, 2011) that a dynamic expression of channel width, linked also to channel gradient, is required to make correct predictions of erosion rate in a transient state. While Finnegan *et al.* (2005) showed, on the basis of the Manning equation, that channel width is proportional to a power d of channel gradient, with $d \approx 0.19$ in steady state conditions, Whittaker *et al.* (2007a) obtained $d \approx 0.44$ for the transient response of bedrock streams to active normal faulting in the Apennines. Moreover, as true bedrock channels with no alluvial cover are rare (Tinkler and Wohl, 1998), investigations of the effects of bed load on the relative adjustment of channel gradient and width have important implications that are still under discussion (Finnegan *et al.*, 2005, 2007; Turowski *et al.*, 2007, 2008; Lague, 2010).

In addition, issues such as the influence of rock resistance on incision are rarely treated in a quantitative way. Even if it does not appear explicitly in the erosion model (see below), rock resistance is generally assumed to be an important control on fluvial erosion and knickpoint migration rate (Sklar and Dietrich, 2001), through spatial variations of the erosivity coefficient of the incision equation. It acts essentially through intact rock mass strength when erosion is dominated by abrasion (Sklar and Dietrich, 2001; Whitbread, 2012), whereas erosion by plucking, in principle mainly controlled by joint spacing, shows in some instances no clear relation with Selby's rock mass strength index (Selby, 1980), possibly because of the additional role of sediment flux (Whitbread, 2012). However, in contrast with the common belief, Roberts and White (2010) were unable to find in their long profile analysis of rivers draining a series of African topographic swells any significant correlation between bedrock lithology and channel gradient or knickpoint location. Likewise, Whittaker and Boulton (2012) concluded from a knickpoint study in the central Apennines and the Hatay graben of southeastern Turkey that their knickpoint migration parameter ψ_A showed little dependence on channel bed rock mass strength.

A few studies have also addressed the role of tributary junctions as possible thresholds in the propagation of the erosion across the drainage network (Crosby and Whipple, 2006; Wobus *et al.*, 2006; Crosby *et al.*, 2007). Indeed, disproportionate junctions (when a migrating knickpoint leaves a large stream to enter a much smaller tributary) are the place of simultaneous changes in many variables. Beyond drainage area, the channel gradient and form, the width/depth ratio, the bed load size and amount, the dominant erosion process, the ratio between bed-form and grain shear stress may all change abruptly, potentially leading to upset the energy balance and, consequently, to alter the migration rate of knickpoints. In particular, even in bedrock channels, the ratio between bed load flux Q_s and transport capacity Q_t, determining the part of stream energy available for bedrock erosion, and, still more, the ratio between bed load D_{50} and river competence, controlling the erosion threshold and the rate of effective discharges, may drastically change across junctions. However, there is so far no clear understanding of how crossing a particular junction toward a tributary may perturb the propagation of an erosion wave.

The Ardennes Plateau is a Paleozoic massif of Western Europe that underwent a middle Pleistocene pulse of uplift. As a result, many Ardennian rivers still exhibit knickpoints or knickzones in their long profile, thus providing an excellent opportunity to investigate how incision models are capable of reproducing the long-term propagation of an erosion wave across an area of moderate relief where multiple environmental influences rapidly interfered with the transient response to the tectonic signal. Furthermore, in its consequences, an uplift pulse should be closer to a sudden base level fall than to the often treated case of a sustained increase in uplift rate. Therefore, the purpose of this study is to examine how far fitting a simple incision model to the Ardennian data set is capable of explaining the distribution of the knickpoints. Subsequently, we attempt to determine the extent to which variables not explicitly accounted for in the basic stream power equation are actually able to explain the misfit between model and observations. In particular, we define a new index providing spatially continuous information about rock resistance to erosion and use it to identify lithological effects on the migration of an incision wave. We also test the potential control of knickpoint trajectory, whose maximum length depends on where a knickpoint leaves the main branches of the drainage network to enter the small tributary through which it will reach a particular place of the catchment divide.

Geological and Geomorphological Setting

The Paleozoic Ardennes Plateau is the western continuation in Belgium of the Rhenish Shield, one of the ancient massifs rising above the NW European platform in front of the Alpine arc (Figure 1). Extending between the Paris basin to the south and **F1** the Cenozoic Anglo-Belgian basin to the north, it is located to the west of the Lower Rhine segment of the European Cenozoic Rift System. The Ardennes massif belongs mostly to the Rheno-hercynian zone of the Variscan fold-and-thrust belt of middle Europe, the northern limit of the present-day plateau corresponding more or less to the Variscan front. Structures
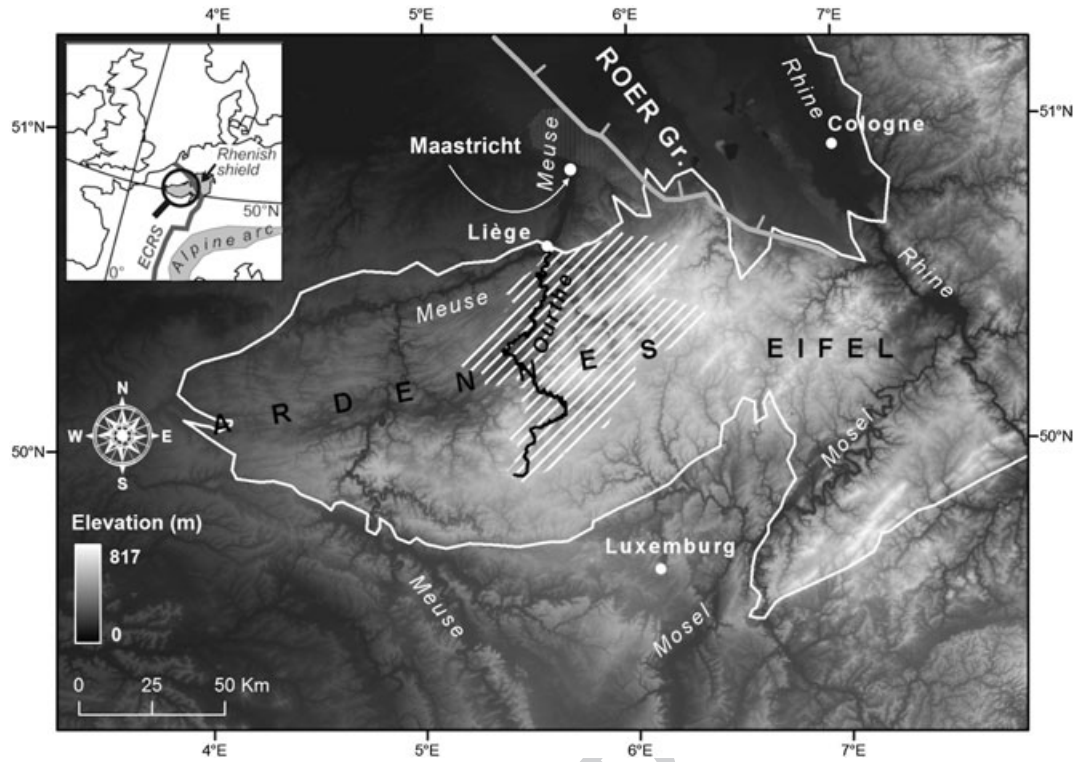
Figure 1. Location of the study area within the Ardennes–Rhenish Shield (delineated in white). The river Ourthe is underlined in black and its catchment is hatched in white. The bold grey line and light grey hatching indicate the approximate location of fault and flexure limiting the en-bloc uplift to the north. In the inset, ECRS stands for European Cenozoic Rift System.

inherited from the Caledonian orogeny and deformed again in Variscan times crop out along the axis of the uplifted massif, and especially in its northeastern part, resulting in a structurally complex basement wherein longitudinal ENE-WSW folds and thrust faults are cut by numerous NW-SE to NNW-SSE striking normal faults.

The deformation of well reconstructed Tertiary planation surfaces and their present-day elevations demonstrate that the Ardennes Plateau underwent a total of 300–450 m rock uplift, locally even more than 500 m in its northeastern part, since the Oligocene, seemingly in response to far-field stresses (Alpine push and Atlantic ridge opening) and possibly also as a consequence of recent mantle upwelling beneath the nearby Eifel (Ritter et al., 2001; Ziegler and Dèzes, 2007). While the development of Neogene stepped surfaces suggests that ~150–200 m uplift already occurred at a very slow pace at this time, numerous studies of the Quaternary terrace staircase in the valleys of the main rivers flowing across the Rhenish shield and the Ardennes (Rhine, Meuse and Mosel), and in those of their tributaries draining the massif, agree on the conclusion that the true uplift of the latter started near the Plio-Pleistocene transition. However, the early Pleistocene uplift rate remained low (≤0.05 mm/yr, as deduced from river incision rates) until the beginning of the middle Pleistocene, when it suddenly increased to reach maximum values of ~0.5 mm/yr in NE Ardennes and Eifel in a pulse between 730 and ~400 ka before coming back to tectonic quiescence (Hoffmann, 1996; Van den Berg, 1996; Meyer and Stets, 1998; Quinif, 1999; Van Balen et al., 2000).

A recent reappraisal of the western Rhenish Shield uplift since 0.73 Ma reduced its maximum amount from previous estimates of ~290 m (Meyer and Stets, 2007) to ~190 m in the SE Eifel and 100–150 m in NE Ardennes, and modified its general shape, namely stretching and straightening its E-W profile (Demoulin and Hallot, 2009). Although the Rhenish Shield as a whole appears as a broad swell, the topographic contrast between the northern Ardennes and its northern foreland is more typical of an en-bloc uplift. There, the border faults of the neighboring Roer graben (Figure 1) accommodate a part of the relative vertical displacement, with estimated ~0.05–0.1 mm/yr individual fault motion rates (Camelbeeck and Meghraoui, 1998; Houtgast et al., 2005) while the deformation of Tertiary planation surfaces shows that the bulk of the uplift is accommodated by a 10- to 20-km-wide flexure zone leading rapidly to the remarkably flat interior of the massif (Demoulin and Hallot, 2009). Based on various morphological observations (vertical spacing between river terraces, timing of stream piracy in the upper Meuse basin, Mosel river sinuosity, geodetic data), Demoulin and Hallot (2009) also suggested that the uplift axis migrated across the massif, from a southern position in the early Pleistocene to a current location in the very northern end of Ardennes and Eifel (which however also recorded the pulse of uplift at 0.73 Ma).

Most of the Ardennes Plateau is drained by rivers of the Meuse basin that have incised 100- to 150-m-deep Pleistocene valleys through it. For more than half a century, numerous field studies have identified a flight of 10–15 terrace levels along the main streams, reducing to 6–7 in their upstream reaches and to 1–3 levels in smaller tributaries (Cornet, 1995; Pissart et al., 1997). According to classical profile reconstructions, such decreasing numbers would have resulted mainly from the upstream convergence of the terraces (Pissart, 1974). However, Demoulin et al. (2012a) recently proposed that they are rather a consequence of knickpoint propagation and diachronic incision. As a consequence of the middle Pleistocene increase in incision rate, valleys in the Ardennes (and in the Rhenish Shield in general) display a typical cross-section that opposes a narrow, steep-sided young valley nested into a broader older valley with gently sloping valleysides carved into the Tertiary topography (Figure 2). Dated from the early Middle Pleistocene **F2** (~0.73 Ma) north of the Ardennes-Rhenish shield (Van den Berg, 1996; Boenigk and Frechen, 2006; Dehnert et al., 2011;
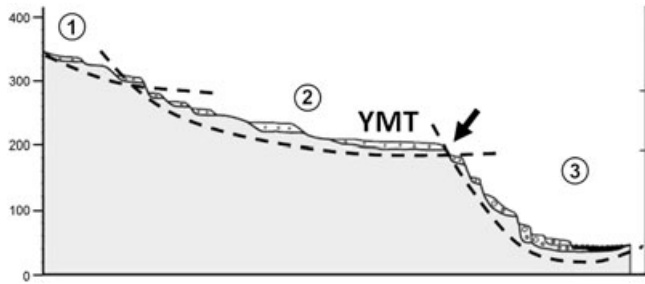
Figure 2. Schematic cross-section of the Ourthe valley showing the marked break of slope (arrow) that corresponds to the onset of the middle Pleistocene incision, with abandonment of the Younger Main Terrace (YMT). Extended terraces are well preserved in the broad early Pleistocene valley (2) carved in the Tertiary paleolandscape (1) whereas the narrow middle Pleistocene valley (3) displays only narrow terraces remnants. This cross-section is typical of most intra-massif valleys.

Rixhon *et al.,* 2011), the extended lower level of the so-called Main Terrace complex clearly separates the two units and marks the beginning of the middle Pleistocene incision episode. Below this key level, a maximum of five much narrower, and vertically closer to each other, younger terraces is more or less well preserved, bearing witness to the continuation of slower incision even after the time of knickpoint initiation and passage. In the lower and middle course of the main Ardennian rivers, the vertical spacing between the lower Main Terrace level (often called the Younger Main Terrace, or YMT) and the next younger terrace amounts to 15–20 m, reflecting the height of the knickzone that started to propagate from 0.73 Ma onwards in the drainage network, and whose present position is marked by knickpoints in the upstream part of the long profiles of many streams. This 'post-YMT' knickpoint generation is the only one recorded in the Ardennes. The propagation of the corresponding erosion wave has been recently confirmed by cosmogenic nuclide dating of terrace sediments of the Meuse, Ourthe and Amblève valleys that traced a diachronic abandonment of the YMT up to the position of the present knickpoint in the Amblève valley (Rixhon *et al.,* 2011). Younger terraces are essentially climatic in origin, their stepwise arrangement responding to synchronous continued profile regradation each time climatic conditions favoured incision after the passage of the erosion wave. They developed as distinct levels only downstream of the knickpoint location of the time because the pre-YMT steady state that still prevails upstream of knickpoints involves no significant incision (Demoulin *et al.,* 2012a).

In this study, we focus on the drainage system of the Ourthe River, the main tributary of the Meuse River in the Ardennes Plateau (Figure 1). The Ourthe catchment (3600 km^2) covers the major part of the NE Ardennes, with a highly asymmetric drainage network characterized by a 150-km-long main stem flowing from south to north very close to the western border of the catchment and two main E-W flowing right-bank tributaries, the Amblève and the Vesdre, which drain the most elevated area (up to 700 m) of the Ardennes (Figure 3(A)). The Ourthe River flows into the Meuse River at Liege, which, at 55 m asl, makes a regional base level located approximately at the northern border of the uplifted massif. The catchment extends mainly over a belt of early Devonian slates surrounding the phyllites and quartzites of the Cambrian Stavelot Massif in the northeast (Figure 3(B)). Except for local rock resistance contrasts, in particular where quartzitic beds crop out, this chiefly slaty bedrock is fairly homogeneous, giving way to alternating middle and late Devonian sandstones, shales and limestones only in the northwestern part of the catchment. There, a 24-km-long reach of the middle Ourthe wanders across a large

depression that was carved ~150 m deep during the Quaternary in Famennian slates highly sensitive to frost shattering. Except for one active fault zone that crosses the Vesdre valley in the NE of the catchment and possibly displaces the river terraces locally, the YMT is not known to have been deformed by recent faulting within the Ourthe basin.
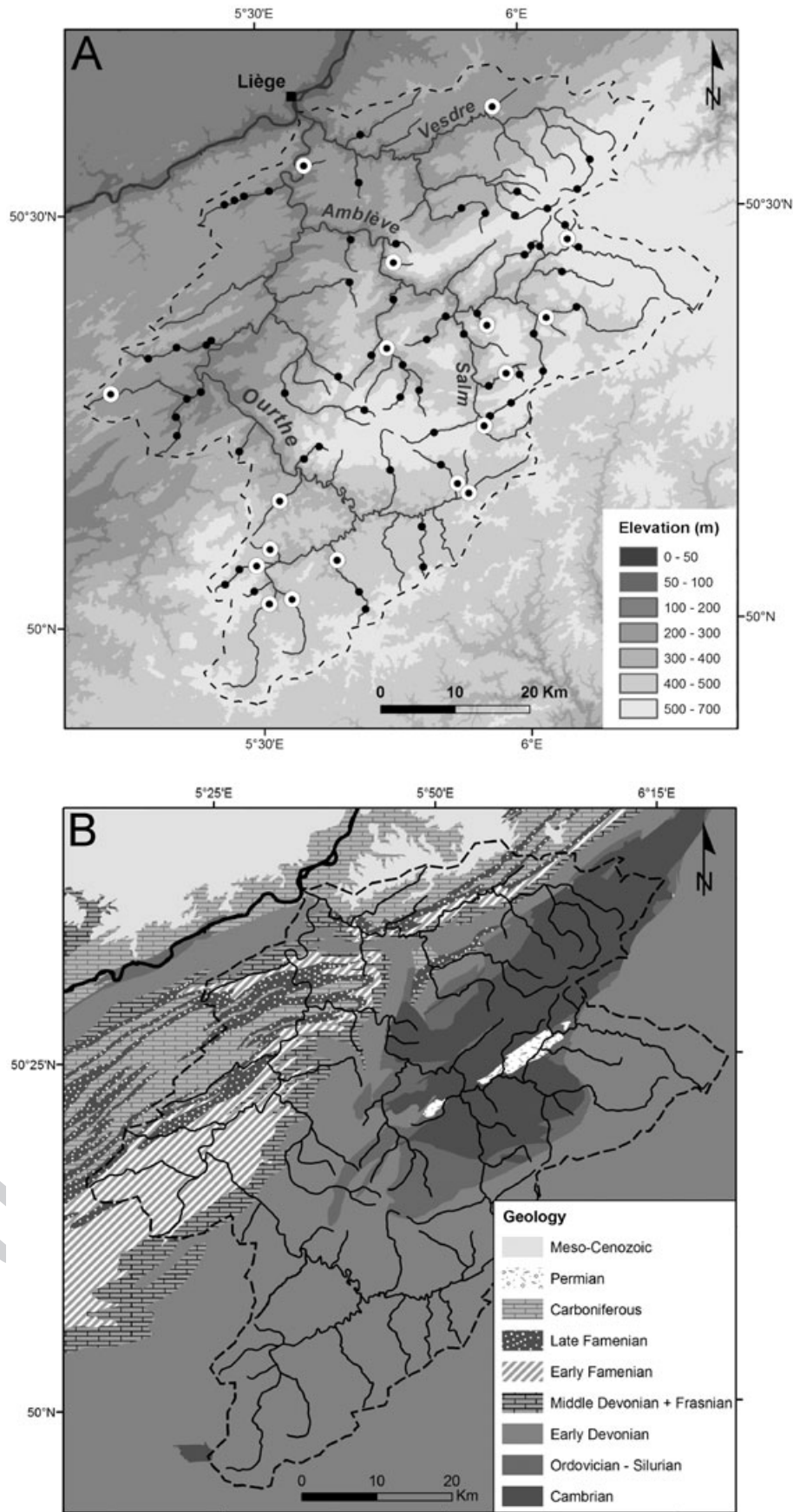
Assumptions about the Relevant Law of Fluvial Erosion

Detachment- or transport-limited model?

Relief of the Ardennes Plateau is low enough to allow the rivers to develop floodplains. Streams of 4th and higher Strahler's orders all currently flow within a well-developed floodplain, suggesting that a transport-limited (TL) model, where erosion rate is limited by the capacity of the river to transport its sediment load, or a mixed model (Whipple and Tucker, 2002) might be best adapted to fluvial erosion in the Ardennian setting. However, whereas this may be true for the lower part of the drainage system at present, it certainly did not hold for the time of incision. The main reason for this lies in the temporal distribution of aggradation and incision through a glacial–interglacial cycle. As shown by the study of many Pleistocene terrace staircases in the valleys of western Europe (Vandenberghe *et al.,* 1994; Antoine *et al.,* 2000; Cordier *et al.,* 2006), the bulk of the terrace deposits is made of coarse sediments accumulated during the cold periods and often overlain by interglacial loams. Within a climatic cycle, incision would occur chiefly during a limited period of time at the warm–cold transition, when annual snowmelt already causes recurring high peak discharges while hillslopes are still covered by vegetation and do not yet deliver much sediment to the valleys: after the rivers cut through their former floodplain (rapidly enough to make the corresponding time span negligible), thus disconnecting their channel from the alluvial cover, they would proceed by incising in the bedrock until the time when periglacial mass transport on bare, frozen, hillslopes begins to supply large amounts of material so that, more than transport-limited, river incision becomes 'transport-impeded' for the rest of the glacial (Cordier *et al.,* 2006; Demoulin *et al.,* 2012a). Therefore, it seems reasonable to assume that, during these brief episodes of incision, river erosion occurred predominantly under detachment-limited (DL) conditions in mixed bedrock–alluvial channels, justifying the use of this kind of model where erosion rates are limited by the capacity of the river to erode its bedrock.

DL incision laws and threshold for erosion

The general form of the most widely used models for bedrock channel incision assumes that the rate of vertical erosion is a power function of some parameter characteristic of the river flow, either (unit) stream power or shear stress (Whipple and Tucker, 1999). Moreover, several authors introduce a critical value of the parameter in the erosion law, which has to be overcome before channel incision can take place (Howard *et al.,* 1994; Tucker and Slingerland, 1997). The nature of this threshold is different depending on which of the main channel incision processes, plucking or bed abrasion (Whipple *et al.,* 2000), prevails. If abrasion dominates, one admits that even the tiniest particle of the bed and suspended loads is able to abrade the channel's bottom, so that no bedrock-controlled threshold has to be considered (Sklar and Dietrich, 2004). Instead, fluvial erosion is then conditioned by a sediment-controlled threshold related to the minimum energy needed

Figure 3. (A) Topography of the study area with the drainage network of the Ourthe River highlighted, showing the distribution of knickpoints in the long profiles of the rivers. Black dots locate all observed knickpoints, circled black dots identify those knickpoints that mark the present position of the post-YMT erosion wave (after Demoulin *et al.*, 2012b). (B) Geology of the study area. Cambrian: quartzites and phyllites; Ordovician-Silurian: mainly schists and phyllites; early Devonian: mainly schists with scattered sandstone levels; middle Devonian+Frasnian: mainly limestones; early Famennian: schists; late Famennian: psammites; Carboniferous; mainly limestones in the Ourthe catchment; Permian: conglomerates overlain by clays; Meso-Cenozoic: chalk and sand.

for sediment entrainment (Van der Beek and Bishop, 2003), which Attal *et al.* (2011) recently showed to be dependent on the median grain size of the sediment. By contrast, when plucking prevails, the threshold for erosion of the channel's uncovered bottom should be mainly bedrock-controlled. However, many field studies concerned with such cases have so far neglected this threshold, arguing that most bed erosion actually occurs for peak discharges involving shear stresses much greater than the critical stress (Howard and Kerby, 1983). As field observations suggest that plucking is the commonest process eroding the intensely jointed and fractured rocks of channel beds in the Ourthe catchment, and in the absence of constraints on erosion thresholds in the study area, we, too, chose not to include such a threshold in our initial analysis, and to come back later to this issue in the light of our modeling results. One should also note that, when testing the ability of various erosion models to predict river incision at the regional scale in the Upper Lachlan catchment (SE Australia), Van der Beek and Bishop (2003) concluded that excess stream power models delivered unsatisfactory results, improving only when the threshold involved tended to zero.

Whatever the underlying physics, the DL models of the stream power family yield the same basic form of the incision law

$$E = K \ A^m \ S^n \tag{1}$$

where the erosion rate E scales with drainage area A and channel gradient S (see Whipple and Tucker (1999) for the developments leading to this equation). K is a dimensional ($L^{1-2m}T^{-1}$) coefficient that includes every variable not accounted for by A and S, notably those of channel geometry, magnitude-frequency distribution of discharge (i.e. climate), rock resistance to erosion, sediment load (quantity and size) and, to some extent, erosion process (Sklar and Dietrich, 1998). The chief difference between the various physical models lies in the values taken by the exponents m and n, respectively $m = n = 1$ in the stream power model, $m \approx 0.5$ and $n \approx 1$ in the unit stream power model, and $m \approx 0.3$ and $n \approx 0.7$ in the shear stress model (Van der Beek and Bishop, 2003). Importantly too, the m/n ratio is a function of parameters defined in the empirical relationships used to obtain Equation (1)

$$\frac{m}{n} = c(1 - b) \tag{2}$$

where b and c appear in the relations respectively between channel width w and water discharge Q for hydraulic geometry

$$w = k_w \ Q^b \tag{3}$$

and between water discharge and drainage area for basin hydrology

$$Q = k_q \ A^c \tag{4}$$

The m/n ratio thus incorporates directly the effects of hydraulic geometry and basin hydrology. The same expression of this ratio is obtained from the shear stress model, though absolute values of m and n are then reduced by one-third.

Improved DL models

In the last 10 years, many variants of the DL model have been proposed, either incorporating refinements in the stream power equation, e.g. more or less complicated sediment load functions (Whipple and Tucker, 2002; Gasparini *et al.*, 2006; Pelletier, 2007), dynamic expression of channel width (Attal *et al.*, 2008; Lague, 2010), and short-term stochasticity of discharge and sediment supply (Lague *et al.*, 2005; Lague, 2010), or formulating a new model for bedrock erosion by abrasion (Sklar and Dietrich, 2004, 2006) and combining it with various sediment load functions (Gasparini *et al.*, 2007; Turowski *et al.*, 2007). However, such models require many data that are rarely available for studies of the long-term response of drainage systems to tectonic signals, so that heavily simplified forms of the stream power law are used in general for knickpoint analysis. Moreover, the saltation–abrasion model of Sklar and Dietrich (2004) in particular, and all models involving a sediment load function in general, are less relevant when erosion by plucking predominates. For these reasons, we chose to adopt the simplest stream power model so that we had not to estimate parameters which are essentially unknowable in the geologic past.

Propagation speed of the erosion wave

If we now turn to the issue of knickpoint migration in bedrock channels, we can start from a slightly rearranged form of the stream power law, written within a reference frame tied to the uplifting catchment

$$\frac{\partial z}{\partial t} = K \ A^m \ S^{n-1} \frac{\partial z}{\partial x} \tag{5}$$

This is an advection equation that yields

$$C = \frac{\partial x}{\partial t} = K \ A^m \ S^{n-1} \tag{6}$$

for the celerity C with which a knickpoint will propagate upstream in the drainage network (K still has dimension of $L^{1-2m}T^{-1}$). If $n \neq 1$, the dependence of C on channel gradient may change the shape of the propagating erosion wave, which in turn may alter the celerity (Whipple and Tucker, 1999). However, when $n = 1$, knickpoint celerity becomes insensitive to channel slope, and the knickpoint migrates upstream at a rate decreasing only as a power function of A and, characteristically, without alteration of form. We then obtain the simplified expression

$$C = K \ A^m \tag{7}$$

Several studies used such an approach to parameterize the stream power equation on the basis of the distribution of knickpoints in a catchment. Berlin and Anderson (2007) adjusted for example this celerity model on the positions of 60- to 110-m-high knickpoints (in fact, waterfalls) distributed in two watersheds of the Roan Plateau, Western Colorado, and they obtained $m = 0.54$ and $K = 1.37 \times 10^{-7}$ m$^{-0.08}$ yr^{-1}. Because of large uncertainties about the initiation time of knickpoint propagation, their modeled K value is disputable. However, the m exponent is less sensitive to this uncertainty and, under the assumption of $n = 1$, its value is in good agreement with the estimates for c ($\rightarrow 1^-$ for everyday flow in small basins) and b (≈ 0.5) usually derived from field measurements (Knighton, 1998). In a study of knickpoint migration in rivers of southern France and in the Nile River in response to the abrupt base level fall that was induced around the Mediterranean Sea by the Messinian crisis, Loget and Van Den Driessche (2009) calculated, without direct reference to the stream power model, that both travel distance and celerity of the knickpoints were power functions of drainage area, with

an exponent comprised between 0·45 and 0·55. In the North Island of New Zealand, where 18-ka-old knickpoints have already reached the headwaters of the Waipaoa catchment, Crosby and Whipple (2006) used a similar celerity formulation, which they applied again without physical reference to the stream power model because the latter assumptions (uniform and steady flow over slopes low enough to allow shear stresses of fluid and sediments to drive incision) are violated at waterfalls. They found that, with a best fit value of 1·125, their exponent on A (equivalent to m) was higher than, but not significantly different from 1. Beside derivation of erosion rates from the dating of fluvial sediments (Anthony and Granger, 2007; Cook et al., 2009; Rixhon et al., 2011), the analysis of the spatial distribution of knickpoints associated with an erosion wave of known age appears therefore to be an efficient tool to provide insight into the details of bedrock channel incision.

Scaling exponent n of channel gradient in the stream power law

We also decided to take $n = 1$ for several reasons. A main argument was that, although they have already traveled far upstream, most knickpoints observed in the drainage network of the Ardennes Plateau have preserved a fairly sharp upper edge **F4** (Figure 4(A)), suggesting that the profile slope break originally created at the margin of the uplifted massif underwent more or less parallel retreat under a prevailing advective component of propagation. In addition, plucking appears to be the dominant channel erosion process in the bedrock streams of the Ourthe catchment, a case in which Whipple et al. (2000) showed that the value of n should also be near unity. These observations thus strongly suggest that n should be roughly 1, so that approximating the wave celerity by Equation (7) seems appropriate. Finally, if n had been left as a free parameter in the modeling, we would have faced the problem of reintroducing channel gradient in the celerity equation while having no reliable gradient data related to the time of knickpoint passage. The less probable $n \neq 1$ hypothesis is thus so far hardly testable and we further note that authors having left n free when fitting the stream power equation to field data had to make other assumptions, like, e.g., fixing $m = 0.5$ (Whittaker and Boulton, 2012).

Input Data: The Knickpoints of the Ourthe Catchment

The post-YMT knickpoint generation corresponds to an incision wave currently approaching completion. Moreover, it responded to an uplift and a resulting increase in topographic relief that did not exceed a few tens of meters in the Ourthe catchment. Therefore, the knickpoints we try to identify, although well marked as many of them still are in the river profiles, never were that high, nor ever so steep as to be in many cases easily distinguished from profile discontinuities of other origin (e.g. rock resistance contrast or tributary junction). This is the reason why we had to be extremely conservative in the knickpoint selection, in order to ensure as little noise as possible in our data set.

The Digital Elevation Model used to produce the river profiles from which the knickpoints were to be extracted is built from an irregular network of points provided by the Belgian National Geographical Institute (IGN). It is comprised of various types of points derived from either direct photogrammetry from aerial photographs at varying scales (1:6000–1/21 000), laser and field data, or the digitization of contour lines
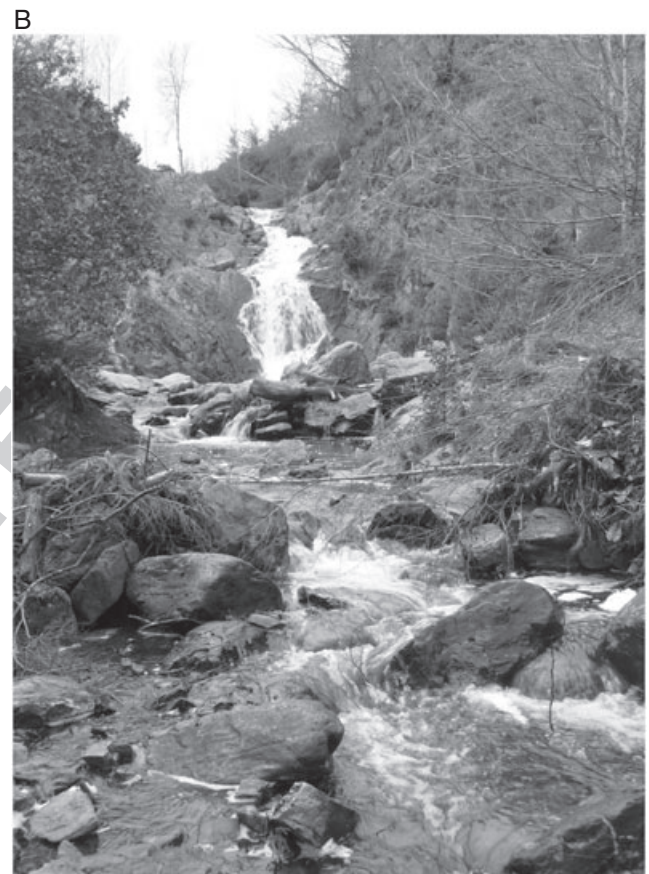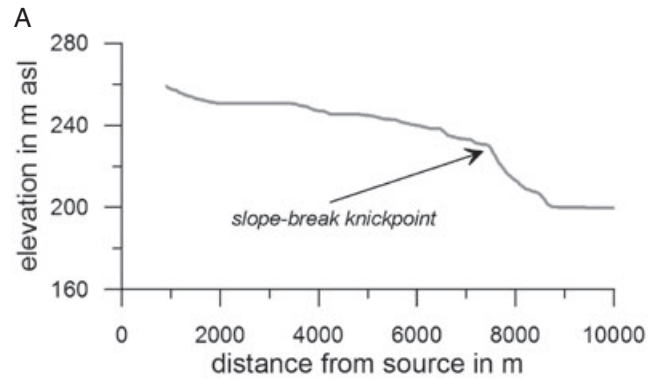

Figure 4. (A) Long profile of the Baelen creek showing the typical slope-break type knickpoint that migrates with the post-YMT erosion wave. (B) Photograph of another knickpoint of the same generation in the Bayehon river.

previously obtained by photogrammetry at 1:20 000 scale. The point RMS errors in (x,y,z) are in the range 0·6–1·6 m and the mean density of the network is ~ 11 points/ha. The DEM was produced at a 20 × 20-m resolution by linear TIN interpolation from this network, additionally constrained by polylines along river lines and watersheds (also supplied by the IGN). The predominance of 5 m contour lines in the elevation data of some areas and the hydrologic correction of the DEM by sink filling often resulted in a jagged appearance of the extracted stream profiles, with frequent 5-m-high and on average 500-m-long steps. Therefore, we smoothed the profiles by resampling the elevation data at stream-wise horizontal 100 m intervals and computing the central moving average of 5-value subsets in order to substantially reduce the noise in the derived profiles of channel gradient (gradient was calculated using a 3-value central scheme). Compared with the approach of Wobus et al. (2006), who recommend selecting data at a regular vertical interval corresponding to the contour line spacing, our data

filtering has the advantages of (1) distributing the filtered data evenly over the river length, and (2) maintaining a higher data density.

A knickpoint is morphologically defined as an abrupt and discrete downstream increase in stream gradient creating a local convexity in an otherwise concave-up equilibrium profile (Anderson and Anderson, 2010). Log-log plots of channel gradient S versus contributing drainage area A, which have been shown to aid the location of knickpoints (Wobus *et al.*, 2006; Berlin and Anderson, 2007), were used to identify knickpoints at places where a local peak in gradient separated river reaches (at least 1 km in length) with different concavity and/or steepness (Figure 5(A)). While small knickpoints with a size similar to the artificial ~5-m-high and a few 100–m-long stairs in the long profiles were filtered out by the smoothing process, the YMT knickpoints, with a ~15–20 m height (see below) over a few 100 m, are preserved and expected to impose local values >15‰ to the smoothed gradients (every gradient data is based on the raw elevation data of a 700-m-long river reach). Such values are much larger than normal channel gradients, which do not exceed 10‰ even in the upstream course of most streams. Practically, knickpoints were thus identified where S/A plots showed local jumps in gradient over the 10‰ level.

We investigated 68 streams of the Ourthe catchment, with drainage sizes ranging from 3600 km² (the Ourthe itself) and 1075 km² (its longest tributary, the Amblève) to a few km². The smallest sampled streams, of Strahler's order 2, are equally distributed throughout the whole catchment. As our script for drainage network extraction set the minimum drainage area to 0.5 km² for a channel to be created, the first data in the S-A plots correspond to drainage areas of about 1 km². Therefore, the break in scaling that is generally noted in response to a change in channel-forming processes around this value (Montgomery and Foufoula-Georgiou, 1993) is not observed here. We recorded a total of 80 knickpoints, but it was immediately obvious, e.g. from the succession of several knickpoints along a single stream, that many of them did not belong to the post-YMT erosion wave (Figure 3(A)). The criteria used to select knickpoints for the final data set were that (1) the knickpoint in the current long profile of a river may be geometrically connected with the upstream prolongation of the YMT profile in this river's valley (Figure 5(B)), (2) their location is not determined by the presence of geological formations identified as very hard rock in the lithological logs of the new geological map of Wallonia (this means that some knickpoints

possibly corresponding to the post-YMT erosion wave but blocked at bedrock resistance contrasts were removed from the data set as a safety precaution), and (3) a knickpoint in a main stream is not located at the junction of a large tributary, where it could simply be caused by a marked contrast between the present bed load/discharge ratios of trunk and tributary, leading to a change in trunk gradient downstream of the junction. The first criterion is especially valuable as it is a positive proof that such knickpoints really result from the propagation of an erosion wave originating from the basin's outlet. Data on the YMT profile in the valleys of the Ourthe catchment were taken from an abundant regional literature (Alexandre, 1957; Ek, 1957; Juvigné and Renard, 1992; Cornet, 1995; Demoulin *et al.*, 2009).

The majority of the 18 retained knickpoints (Figure 3(A)) belong to the slope-break type as defined by Lague (2014) (Figure 4(A)). They are now approaching the headwaters of the Ourthe catchment, being a maximum 20 km from the drainage divide, and in some cases less than 2 km from the source of the smallest streams (Table I). They have traveled distances ranging from ~14 km in small creeks joining the Ourthe very close to the basin's outlet to 145 km along the main stem. As deduced from the vertical spacing between the YMT and the next youngest terrace in the Ardennian valleys, they generally are around 20 m high, but their moderate gradient ($0.01 < S < 0.1$), gradually merging in the graded profile downstream, makes some of them inconspicuous in the field. Moreover, many of them exhibit gravel beds bearing witness to the current absence of incision. Such a faded appearance is explained by the widely acknowledged fact that, in the midst of an interglacial, rather low and infrequent peak discharges are not favourable to incision and the alluvial material of the last glacial still clutters up the valley bottoms.

Modeling the Propagation of the Post-YMT Erosion Wave

Parameterization of the stream power law

The numerical model we use relies on Equation (8), considering that after an incision pulse is initiated at the catchment's outlet, an erosion wave propagates upstream within the entire drainage network at a rate that is a power function of the
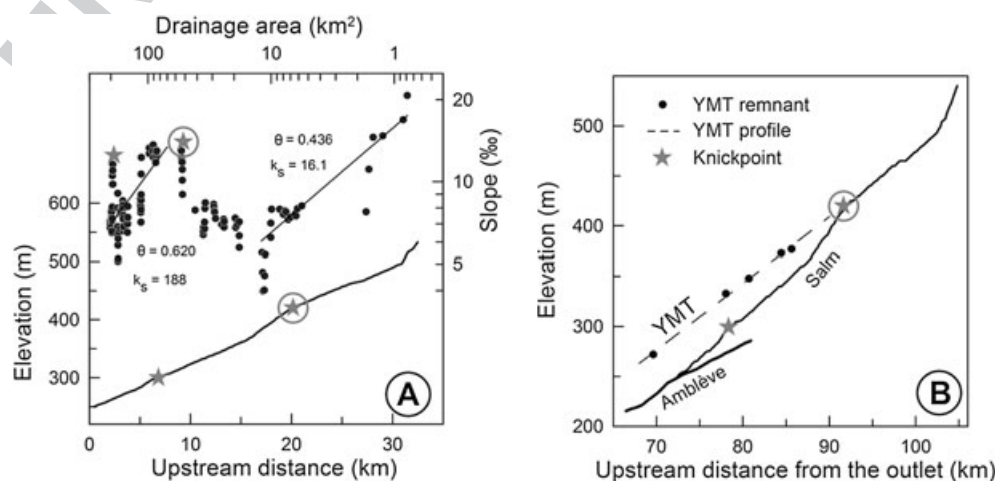
Figure 5. (A) Log(S)–log(A) plot (black dots) of the Salm River (see location in Figure 3), showing the location of a knickpoint (circled star) separating two reaches of distinctly different concavity and steepness; bottom of the graph: location of the observed knickpoints along the river's long profile. (B) Long profile of the current Salm channel and of the YMT preserved in its valley, showing that the knickpoint located in the present-day profile by the circled star marks indeed the position reached by the incision wave that caused the abandonment of the YMT (after Demoulin *et al.*, 2012b).

Table I. Knickpoints locating the position reached by the post-YMT erosion wave in streams of the Ourthe catchment

Stream	Distance from Liege (km)	Distance from divide (km)	Drainage area at KP position (km^2)
Baelen	46,1	7·7	13·4
Basseille	140,3	9·6	24·3
Bayehon	99,7	7·3	9·7
Bouen	78,7	2·2	2·7
Bronze	101,5	7·7	11·1
Chavresse	13,6	4·3	3·0
Chefna	52,8	4·4	4·7
Cherain	143,0	9· 8	29·2
Heure	86,7	4·7	6·7
Laval	145,8	14·8	69·5
Lienne	71,0	13·4	81·3
W Ourthe	145,3	20·0	95·9
E Ourthe	142,4	12·5	39·9
Petit-Thier	90,7	6·4	11·4
Rahimont	130,1	13·9	46·6
Robas	91,6	5·6	8·2
Salm	92,8	13·1	35·7
Tenneville	139,5	5·0	9·0

contributing drainage area. We thus consider drainage area as the key variable and explore the coefficient and exponent on it, assuming first that they remain constant over the entire study area. Working with the 20x20 m square grid of the DEM, the model calculates the time needed by a knickpoint i to move in the drainage network from a grid point j to the neighbor point $j-1$, to which a fixed A_{j-1} (the area drained at the entrance in the grid point j) is associated

$$\Delta t_{i,j} = \int_{i,j}^{i,j-1} \frac{-1}{K A^m} dx \approx \frac{1}{K A_{i,j-1}^m} \left(x_{i,j} - x_{i,j-1} \right) \quad (8)$$

$(x_{i,j} - x_{i,j-1})$ being either the straight line or diagonal distance across the cell (Demoulin et al., 2012b). The time needed for the erosion wave to reach any point n in the drainage network is then given by

$$t_{i,n} = \sum_{j=j_{outlet}}^{n} \Delta t_{i,j} \quad (9)$$

Particular values of K and m are defined at the start of each model run. To constrain these parameters, we classically used

the brute force two-parameter search first advocated by Stock and Montgomery (1999), with a 300x300 search matrix, m varying linearly between 0.2 and 1·3, and K logarithmically between 10^{-12} and 10^{-3}. We assumed that the erosion wave started to invade the Ourthe catchment at 700 ka, noting that uncertainty on this age impacts the modeled value of the erosivity coefficient K in direct proportion, but hardly affects the best fit m.

Because of the current location of the erosion wave near the headwaters, the strongly reduced rate of knickpoint migration makes the model adjustment much more sensitive to time than to position. Therefore, following Demoulin et al. (2012b), we used a time-based misfit function searching to minimize the sum of squared differences between 700 ka and the modeled times at which the knickpoints should have reached their actual location. In other words, we searched for the (m, K) couple that minimized the variability of the knickpoint travel times around 700 ka. In this case, a negative time residual means that the knickpoint needed less time than predicted to reach its current position, thus that it migrated faster than expected. Distance residuals may of course also be calculated from such an adjustment by applying the time-based best fit (m,K) couple for t = 700 ka, and have a reverse sign behavior. Indeed, as the distances are measured positively from the catchment's outlet towards the headwaters, a knickpoint propagating faster than predicted is located upstream of its modeled position and displays therefore a positive distance residual.

Our best fit (m, K) couple yielded m = 0·75 and K = 4·63 × 10^{-8} m$^{-0.5}$y^{-1} (Figure 6(A)). We used the parameter **F6** ranges corresponding to all misfit values comprised within 4% of the minimum misfit as a quality indicator of the adjustment, so as to be able to compare our figures with those found by Berlin and Anderson (2007) in the Roan Plateau (Colorado). The ranges obtained are 0·69–0·81 for m and 1·43 × 10^{-8} – 1·61 × 10^{-7} for K, indicating that the adjustment quality is similar to that in the Roan Plateau (0.50 < m < 0.62; 3·33 × 10^{-8} < K < 2.87 × 10^{-7}). While the m range is satisfactorily narrow, that of K extends over one order of magnitude, indicating that the fit is much less sensitive to K than to m. Time residuals of the adjustment amount to a mean 68 ka and a standard deviation of 178 ka (Figure 6(B)). Together with the large K range, this suggests that fitting a unique K value might not be optimal and that the effect of spatially varying controls on K should be investigated (see below). Mean and standard deviation of the corresponding distance residuals are respectively –0.8 and 2.3 km. Expressed as a percentage of the distance actually traveled by a knickpoint, the mean distance residual amounts to 2.5%, and even 1.5% if we exclude two extreme values. This shows that, despite
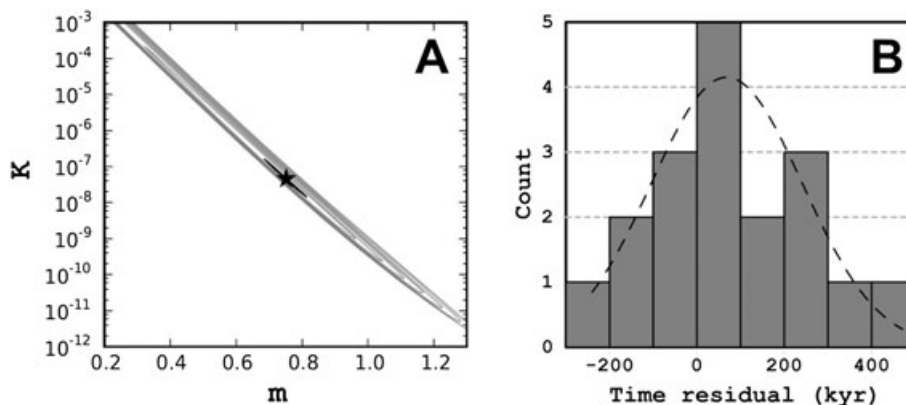
Figure 6. (A) Contours of time misfit for the knickpoint celerity model run over a 300 × 300 (m, K) search matrix. The star indicates the best fit (m, K) combination. The bold black contour encompasses misfit values comprised within 4% of the minimum misfit. (B) Statistical distribution of the time residuals. The dashed line shows the associated normal distribution.

apparently large time residuals (but remember that, for drainage areas of ~10 km^2, a ~13 ka time residual is equivalent to only 0·1 km distance residual), the model satisfactorily accounts for the first-order characteristics of the knickpoint spatial distribution. The residual distributions are not significantly different from gaussian and consistently show that, on average, the knickpoints are somewhat delayed with respect to the model, lagging often 1–3 km downstream of their expected position. In the detail, 12 of the 18 actual knickpoints are located downstream of their model forecast, some of them showing delays of several 100 ky especially in very small streams of the downstream half of the **F7** catchment (Chavresse, Baelen, Chefna) (Figure 7). Knickpoints present in the five smallest streams (watershed ≤ 15 km^2) are all delayed with respect to the model, from 54 ky in the Bayehon up to 470 ky in the Chavresse, and systematically stay not more than 2 km upstream of the junction. As the knickpoint celerity is extremely low in such streams, their large time residuals are however associated with much smaller distance residuals **T2** (Table II). The knickpoint most ahead of its predicted counterpart (240 ky) is observed in the Heure River, in the westernmost part of the Ourthe catchment

Controls on knickpoint retreat contained in the model residuals

Despite the good quality of the model fit, the time residuals appear rather contrasted in value and their spatial distribution is not random, with a majority of larger positive residuals present in the downstream (northern) half of the catchment (Figure 7). This raises the central issue of how realistic it is to derive unique m and K values for the entire study area in spite of spatial variations of factors such as, e.g., rock resistance to fluvial erosion. Residual analysis provides an opportunity to check for the effect of spatially heterogeneous variables. Therefore, we tried to extract such hidden information by searching for correlations between the residuals and empirical estimates of various variables potentially affecting knickpoint behavior.
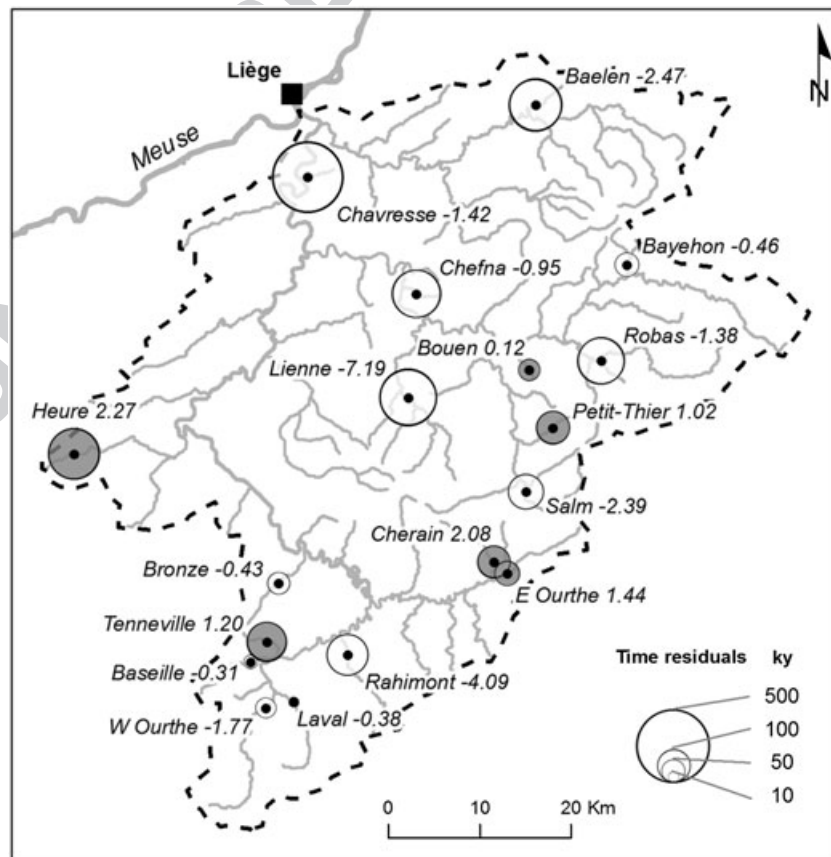
Table II. Time and distance residuals of the celerity model adjustment, rock resistance index values (see definition in the text), and local steepness values (with $\theta_{ref}=0.55$) for the knickpoints of the Ourthe catchment

Knickpoint	Time residual (ky)	Distance residual (km)	Rock resistance index	Local steepness at KP
Baelen	262,457	-2,467	0·048	250
Basseille	17,381	-0,307	0·277	175
Bayehon	53,916	-0,463	-0·051	230
Bouen	-42,969	0,12	-0·141	140
Bronze	45,874	-0,434	0·323	210
Chavresse	470,245	-1,417	-0·066	315
Chefna	217,985	-0,949	-0·139	465
Cherain	-97,020	2,078	0·130	115
Heure	-240,016	2,274	0·109	60
Laval	9,734	-0,378	0·274	225
Lienne	304,940	-7,193	-0·235	224
W Ourthe	38,166	-1,767	0·289	210
E Ourthe	-56,632	1,44	0·136	165
Petit-Thier	-100,244	1,022	-0·199	165
Rahimont	161,481	-4,048	0·222	280
Robas	208,306	-1,382	-0·078	255
Salm	116,669	-2,386	-0·153	200
Tenneville	-141,369	1,201	0·236	130

Figure 7. Spatial distribution of the knickpoint time residuals (in ky). Open circles denote delayed knickpoints, solid light grey circles knickpoints ahead of their modeled position. The numbers following the stream names give the corresponding distance residuals in kilometers.

Beyond drainage area and channel gradient, accounted for by the basic stream power equation (see section 'Scaling exponent n of channel gradient in the stream power law' for the justification of our choice of n = 1, which lets channel gradient disappear from the celerity equation), and acknowledging the absence of significant orographic effect on rainfall depths in the Ourthe catchment, the following variables might be considered: (1) spatially variable erodibility of the bedrock, (2) spatially non-uniform uplift rate, (3) tributary junctions, which may be envisaged as sensitive points in the propagation of erosion through the drainage network, (4) bed load quantity and grain size, and (5) channel width. Moreover, as the spatial distribution of the model time residuals is far from random (Figure 7), the possible effect of location in the drainage system is also worth exploration.

As the knickpoints have traveled far upstream and move now at reduced speed, as most of them are currently inactive due to unfavorable climatic/hydrologic conditions (the interglacial discharge regime of the Ardennian rivers is such that most of them are still struggling with evacuating the gravel stock accumulated in their valleys during the last glacial), there are no longer means of estimating the bed load characteristics and the channel width that were associated with knickpoint propagation during episodes of active incision, so that we cannot treat the effect of these variables directly through residual analysis. The dominantly en-bloc character of the NE Ardennes uplift since the middle Pleistocene (according to the uplift map of Demoulin and Hallot (2009), the tilt component associated with the uplift pulse that cause knickpoint initiation did not exceed 0.2‰) further allows us to neglect spatial variations of uplift rate within the Ourthe catchment (uplift rate does not anyway control knickpoint celerity in case n = 1). Therefore, as we could not find meaningful proxies for the possible junction crossing effect, we limit our investigations to two less elusive parameters, namely rock erodibility, which obviously affects erosion rates but is difficult to quantify, and location in the drainage system, which we believe deserve exploratory work.

Rock resistance
Resistance of channel bedrock to erosion is often regarded as one important control on fluvial incision that is contained in the coefficient of the stream power equation (Sklar and Dietrich, 2001). Yet, large ranges of strength (from weak shales to hard quartzites and arkoses) and joint spacing (from closely spaced cleavage through variously spaced jointing to thick massive layers) are displayed by the rocks exposed in the Ourthe catchment, resulting in numerous spatial changes in rock resistance. Therefore, we first examine to what extent model time residuals may be explained by this factor.

Although Selby's rock mass strength index (Selby, 1980) is often used as a proxy for the lithological variable (Whittaker *et al.*, 2008), it requires numerous field measurements and its values nevertheless retain a marked local influence that makes interpolation or generalization equally biased (think of, e.g., the effect of continuously changing angle between channel axis and joints within a given rock formation). We preferred therefore to build a proxy for rock resistance to erosion based on a measure of the large-scale effect of lithology on the landscape. An objective and physically meaningful measure may be obtained from the rock volumes eroded since abandonment of the YMT, which explicitly link the calculated index to the resistance of the rocks carved by the propagating erosion wave. Indeed, a similar approach was recently employed for the same purpose by Whitbread (2012) calculating what she called reach-scale erosion fluxes and showing that these fluxes are highly correlated with Schmidt hammer measurements of intact rock strength. We used YMT field data and the YMT profile

recently interpolated by Demoulin *et al.* (2009) over the entire Ourthe catchment to estimate the rock volumes (V_{obs}) eroded per 200-m-long valley segment since abandonment of the terrace. These volumes were obtained by subtracting the current topography from the topography reconstructed for the time of the YMT (Figure 8(A)). The spatial variations of eroded volumes **F8** respond however not only to changes in bedrock erodibility, mainly through variations in valley width, but also to the downstream increase in eroding power of the rivers and erosion time since the knickpoint passage. To remove the latter effects, we searched for correlations between eroded rock slice and several variables describing position within the drainage network. The best correlation was obtained for the following exponential relation with distance L_{down} to the basin's outlet ($r^2 = 0.39$, n = 16083) (Figure 8(B)):

$$V_{mod} = 291938 * \exp(-0.0000159 * L_{down}) \qquad (10)$$

By contrast, scaling for example the eroded volumes with $A^{0.5}$ resulted in no correlation ($r^2 = 0.05$), while the best power function between V_{mod} and $A^{0.35}$ explained only 27% of the volume variance. Next, we tested two formulations of a local rock resistance index derived from the remaining volume anomalies and expressed as the cube root of the ratios ($V_{obs} - V_{mod})/V_{mod}$ and V_{obs}/V_{mod}, in order to come back from volume to distance scaling. In passing, note that the continuous character of such easily accessible, DEM-derived proxies for rock resistance also allows them to be considered for inclusion from the beginning in the modeling of knickpoint propagation (though the index definition restricts its mapping to the part of the network already traveled by the erosion wave) (Figure 8(C)). In the residual analysis performed hereafter, we however needed to associate a unique proxy value with each particular knickpoint. These values were obtained simply by averaging either local index values over the total distance traveled by the knickpoints.

Location in the drainage system and knickpoint trajectory
The spatial distribution of model time residuals in the Ourthe catchment displays a clear systematic component (Figure 7). Indeed, most large positive residuals, betraying highly delayed knickpoint migration, are observed in small to very small streams located in the downstream half of the catchment, suggesting that knickpoint trajectory and, as a result, the present knickpoint location might be responsible for a part of the residuals. Therefore, whatever the underlying cause, we want to examine how much various explicit position indicators (independent of drainage area, already accounted for by the stream power equation) might explain these residuals. We search for correlation between time residuals and the following variables: total (outlet to divide) length L_{tot} of knickpoint trajectory, travel distance L_{out} from outlet to knickpoint's present position, and distance of current position of knickpoint to divide L_{div}.

Results
As illustrated by Figure 8(C), rock resistance estimates derived from the proxy based on eroded volumes are remarkably consistent with the qualitative estimates of bedrock erodibility deduced from the lithological information provided with the new geological map of Wallonia, showing that this proxy provides a faithful representation of rock resistance variations. However, none of the two tested rock resistance indices revealed correlation with the model time residuals. The least weak relation was obtained on the basis of the mean of local anomalies expressed as $[(V_{obs} - V_{mod})/V_{mod}]^{0.33}$ but, with $r^2 = 0.13$ (n = 18), it is statistically nonsignificant even at the 90% confidence level ($P = 0.14$) (Figure 9(A)). One will note **F9**
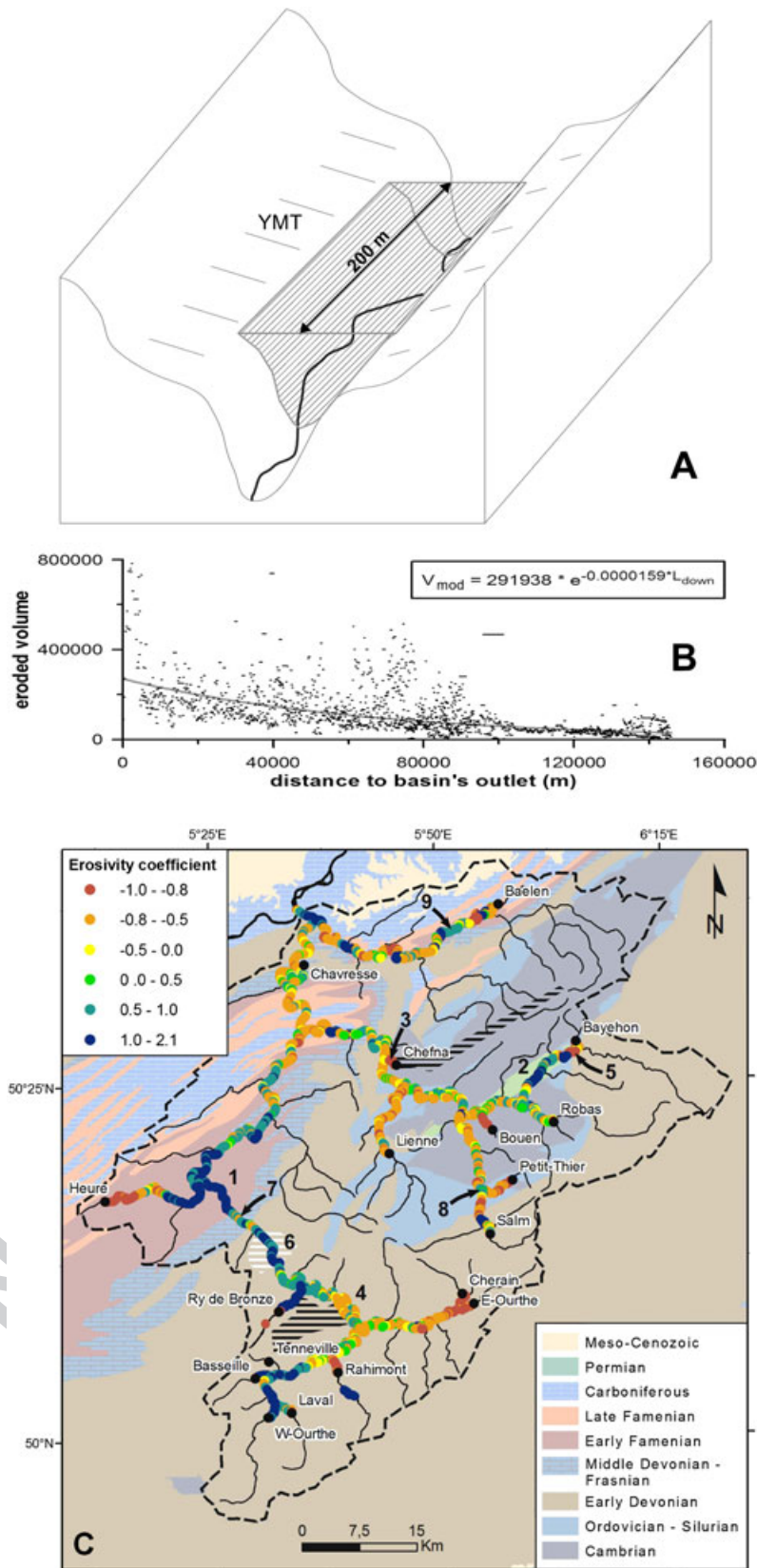
Figure 8. (A) Sketch illustrating how the volume of post-YMT valley erosion – a proxy for rock resistance – is calculated per 200-m-long valley segment. (B) Relation expressing the control of position in the drainage network, best described by the distance to the basin's outlet, on post-YMT valley erosion. (C) Map of rock resistance variations along the paths followed by the studied knickpoints, based on the cubic root of the normalized volume residuals (after removal of the position effect according to the relation shown in (B)). Circles colored in cold (blue) tones denote zones of excess erosion, i.e. low rock resistance, warm colours denote zones of restrained erosion, i.e. harder bedrock. Background colours refer to the geology, supplemented by black or white hatching respectively for harder or weaker rock layers or formations. Numbers identify exemple zones where rock resistance proxy values are clearly consistent with the known relative erodibility of the bedrock: weak schists of the early Famennian (1); weakly cemented conglomerates and clays of the Permian (2); hard quartzites of the Vecquée ridge (Cambrian) (3); relatively harder sandstones of the Pernelle Formation (upper Pragian) (4) included in the softer schists and phyllites of the La Roche Formation (middle Pragian) (6); hard arkoses of the lower Lochkovian (5); Givetian limestones (7), slighty harder than the surrounding schists; locally weaker schists of the lower Tremadocian (8) and the Frasnian (9). This figure is available in colour online at wileyonlinelibrary.com/journal/espl
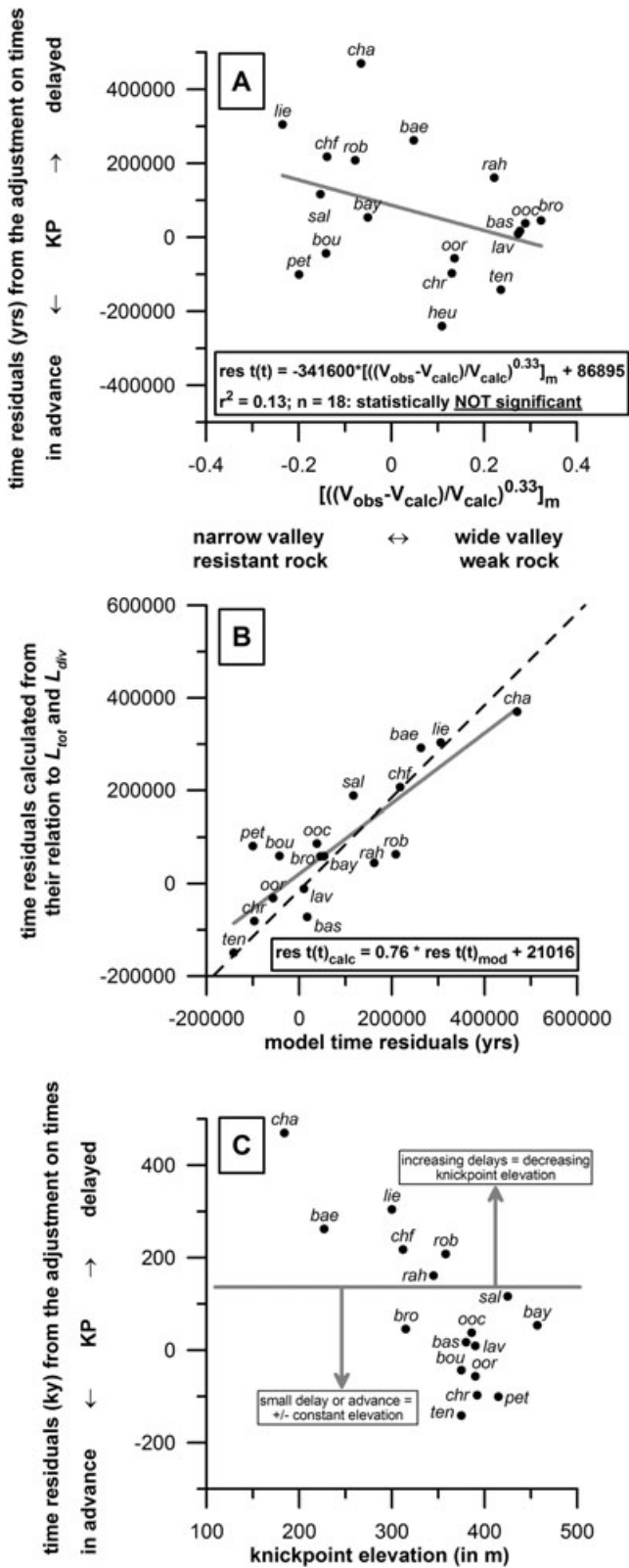
Figure 9. Regression of (A) time residuals of the stream power model fit on the rock resistance index $[((V_{obs} - V_{mod})/V_{mod})^{0.33}]_m$ (see text for explanation), (B) of the time residuals calculated from their relation to two position variables (see text for detail) on the model time residuals, and (C) of the model time residuals on knickpoint elevation. The regression coefficient of 0.76 in (B) represents the percentage of model time residual variance explained by the two position variables; the vertical distances to the (1:1) dashed line represent the remaining time residuals after removal of the position effect. Graph (C) shows that the rule of uniform knickpoint altitude (Niemann et al., 2001) is satisfactorily met except for the six knickpoints with the largest propagation delays.

in passing that correlation between rock resistance index and distance residuals (as obtained from time adjustment) is still weaker in all cases, which is due to the fact that a particular time lag (or advance) in knickpoint propagation has a different impact on traveled distance depending on the place where it occurs and on the knickpoint celerity in that place, so that time and distance residuals are only moderately correlated. However, an analysis of variance (ANOVA) unequivocally showed that the mean rock resistance index is significantly different between the paths followed by each knickpoint (Fischer $F_{calc} = 265.24 >>> F(95;17;76508) \approx 1.61$).

By contrast, model time residuals display clear links with all knickpoint trajectory proxies, and we found that up to 76% of the residual variance is explained by a multiple linear regression of time residuals on two distance variables, namely the total knickpoint trajectory length L_{tot}, which accounts for 52% of the variance, and, secondarily, the distance of current position of knickpoint to divide L_{div} (Figure 9(C)). In particular, time residuals are negatively correlated with trajectory length. Moreover, trajectory proxies show an almost as good correlation with the distance residuals of the time-based model fit.

Discussion

Bedrock resistance and knickpoint migration rate

Once freed from discharge and time effects, both controlled by position along the river, rock volumes carved by valley deepening and widening at and following the passage of an erosion wave are a representative global *a posteriori* indicator of the rock mass resistance factor of erosion (Figure 8(C)). Indeed, it objectively expresses the result of a combination of several resistance-controlling parameters, notably fresh bedrock strength, degree of weathering, joint spacing, structural attitude with respect to changing stream orientation, contrast in resistance between local bedrock and abrading bed load. As resistance variations seem to often cause much more contrasted responses in lateral than vertical fluvial erosion, including the former in the indicator's definition increases its ability to highlight these variations. Moreover, the spatially continuous record of rock resistance effect prevents generalization issues.

The absence of correlation between time residuals and proxys for rock resistance in the Ourthe catchment is rather surprising at first glance. An explanation might have resided in that variations in bedrock lithology would have been greater along a single knickpoint's path than in average between different paths. However, an ANOVA analysis revealed the contrary, showing that the index values for mean rock resistance differ significantly between the paths followed by the knickpoints. Each particular path has a specific rock resistance fingerprint.

Therefore, the absence of evidence for a link between model time residuals and any proxy for rock resistance despite the latter's variability (Table II) leads us to propose that, over the long term, bedrock resistance exerts only a limited effect on knickpoint migration rate and the associated vertical erosion, in stark contrast with its strong control on lateral erosion. This may be particularly true here because of the short duration of the uplift pulse and the correspondingly limited amount of transmitted incision, but the common occurrence of deep gorges cut in resistant rocks points in fact to the much broader significance of this conclusion. It especially holds for settings similar to the Ardennes, characterized by not far from random patterns of rock resistance that considerably narrow the range of knickpoint paths' mean rock resistances. However, in regions where rock resistance contrasts are not distributed randomly, but rather oppose large areas underlain by very

different bedrocks, not only would it not make sense to estimate a unique relation between resistance index and streamwise distance in order to remove the position effect on eroded volumes, but the index values would also be much more regionally contrasted and locally uniform, so that the regional rock resistance control on erosion would have more chances to emerge. Nevertheless, our conclusion is supported by similar findings of Roberts and White (2010) in Africa and Whittaker and Boulton (2012) in Italy and Turkey.

While all these observations converge to show that rock resistance has a limited impact on tectonic knickpoint behavior, the existence of lithologic knickpoints (Figure 3) demonstrates that it nevertheless imprints the way stream erosion proceeds. Lithologic knickpoints are permanent anchored features that keep expressing rock resistance contrasts in equilibrium profiles, in which local channel steepening compensates for the additional energy required to erode stronger bedrock. As a result, the (locally irregular) pre-uplift steady state profile is already in equilibrium with rock resistance variations, and the migrating tectonic knickpoint travels over lithologic knickpoints with no or minimal rock mass strength effect on its migration rate.

Knickpoint trajectory and migration rate of the erosion wave

The predictive power demonstrated by trajectory proxies is much more convincing. Not only are 76% of the time residual variance explained, but the fairly uniform distribution of the data across the ranges of the independent variables moreover provides a high quality correlation. In this respect, we note first that the Heure knickpoint appears as an outlier in all significant correlations between time residuals and these variables (e.g. -2.6σ in the retained multiple regression). While we have no simple explanation for the exotic behavior of this knickpoint, we decided to remove it from the residual analysis. We also stress that trajectory proxies primarily refer to the path length followed by the knickpoint from outlet to a particular place of the catchment's divide. In other words, their value essentially depends on the place where the knickpoint leaves the main branches of the drainage system to venture into a very small tributary (with Strahler order generally ≤ 2) and is not determined by the model distance residuals.

The largest delays in the erosion wave propagation, possibly indicative of the latter's more or less long stopping, are observed in general where a high-amplitude knickpoint enters an abruptly smaller tributary valley. Actually, this occurs mostly in the downstream part of the basin, i.e. for small knickpoint trajectories (Figure 7), where the recorded delays are all the longer as the erosion wave reached such places early in the course of its upstream migration. As an example, we observe that the delay suffered by knickpoint migration in the Chavresse is very high because the short trajectory length (~18 km, see Table I) implied that the erosion wave entered this small creek, where its propagation was stopped, very early (Figure 7). By contrast, the knickpoint currently observed, e.g. in the Tenneville creek, to which a much longer trajectory (~145 km) is associated, had to travel a long way obeying the modeled simple stream power law before it entered a tributary in which it might encounter an erosion threshold and be delayed.

Interestingly, the vertical distribution of the knickpoints tells the same story. According to Niemann *et al.* (2001), the simple stream power model predicts that the knickpoints set off by a given event should travel vertically at the same rate, so that, at any time, they are at similar elevations. Here, while the

knickpoints with no or negative delay lie indeed in a narrow range of elevations around 400 m, the others show a strong negative correlation between positive time residuals and elevations below 400 m (Figure 9(D)).

The fate of knickpoints in these small streams of the middle and lower Ourthe catchment recalls to some extent what has been described by Crosby and Whipple (2006) as hanging valleys in New Zealand. According to them, not to exceed a critical drainage area would be a necessary, but not sufficient, condition for producing hanging valleys. In NE Ardennes, only streams with $A < 10$ km^2 display a clear hanging character (Chavresse, Chefna), but by far not all such small streams are hanging valleys with delayed knickpoints (e.g. Tenneville, Bouen, and other streams where knickpoints are no longer observed). A measure of the channel profile steepness k (Equation (12)) of the reach downstream of the knickpoint is probably a better indicator of the potential hanging character of a valley, with values > 300 for unequivocal hanging valleys in NE Ardennes (Table II). Sklar and Dietrich (2004) showed that, in the process of bedrock abrasion by saltating bed load particles, the highest transport stages of a river might be less erosive than more moderate stages because of the decreased frequency of particle impacts on the channel bed. Based on this, Wobus *et al.* (2006) conceptually defined the conditions needed for hanging valleys to develop and Crosby *et al.* (2007) theorized about it in the frame of a sediment flux-dependent incision model. They argued that erosion rates decrease when the channel gradient steepens beyond some threshold, or the low sediment flux response of a tributary prevents it keeping pace with the main stem incision. These are situations that have chances to happen especially at the mouth of small tributaries joining the main stem, where a second threshold, namely in the rate of main stem lowering, should also be exceeded so that the tributary gradient may become sufficiently oversteepened and a hanging valley is created. In their Taiwanese case study, Wobus *et al.* (2006) measured gradients higher than 0.28 for the oversteepened lower reach of the hanging valleys, often leading to the development of waterfalls and thus, to a change in erosion process that might be partly responsible for fixing the erosion wave near the mouth of these streams.

By contrast, in the Ourthe catchment, although local up to 8-m-high waterfalls may exist, the patent hanging valleys display lower channel gradients, mostly in the range 0.08–0.1, suggesting that knickpoint migration may be impeded in small streams independently of a radical change toward waterfall retreat controlled by rock strength. We note also that prevalence of plucking makes the Ardennian case different from those in New Zealand and Taiwan. The relation between model time residuals and knickpoint trajectory length in fact leads us back to the role of junctions. It shows that time residuals are not related to some characteristic of the junctions but rather to the *time*, depending on trajectory length, at which the significant junction was crossed. This suggests that, from that time onwards, an erosion threshold was rapidly reached, which stopped the progression of the erosion wave in the small tributary or hanging valley past the junction. However, unrelated to the model time residuals, the variables defining such an erosion threshold cannot be discussed on the basis of our data set. We just feel from sparse field observation that, in tributaries preserving highly delayed knickpoints, large across-junction changes in the bed load grain size/stream competence ratio might have been determining, and deserve further specific research effort.

In any event, this implies that adjusting the simplest form of the stream power law to a knickpoint data set affected by the existence of an erosion threshold over-estimates knickpoint celerity especially in small to very small streams, and that all

refinements offered by more elaborate, and thus much more difficult to handle, erosion equations (including sediment flux function, incision threshold, discharge stochasticity) probably would not change much the observed large delays in knickpoint migration as long as the erosion threshold is kept uniform. At least in the special case of an advanced erosion wave with knickpoints observed in the smallest branches of the drainage system, and in accordance with the bed load grain size control on erosion rate recognized by Attal *et al*. (2011), improved model fitting should pass through the introduction of a spatially varying, bed load grain size-dependent, threshold in the analysis. While collecting bed load D_{50} data over a whole catchment is probably unrealistic in most cases, a pragmatic way of addressing this threshold issue might be to determine whether there exists a drainage size across which bed load D_{50} changes abruptly. In this respect, it is worth noting that almost all Ardennian knickpoints with migration delays 200 ka are blocked at places with $A \leq \sim 10$ km^2, which is also the drainage area associated with the maximum coarsening of the bed load observed by Brummer and Montgomery (2003) in mountain drainage basins of western Washington.

Meaning of the modeled m and K values

Under the safe assumption that the knickpoints (observed in all cases for $A > 2.5$ km^2) have not yet reached the headwater reaches where channel evolution may be dominated by non-fluvial processes, the simple stream power model satisfactorily fits the knickpoint data of the Ourthe catchment for values of the m exponent of drainage area around 0.75, which also corresponds to m/n = 0.75 under the assumption that n = 1. The quality of our fit is comparable with what has been obtained in similar exercises carried out in other parts of the world and the parameter values are also consistent with figures derived elsewhere (Crosby and Whipple, 2006; Berlin and Anderson, 2007; Loget and Van Den Driessche, 2009). Although size and scatter of the time residuals of the adjustment may appear large, they correspond to fairly small distance residuals and especially owe their characteristics to the current location of the knickpoints high in the catchment, where celerity is very low, making thus time a highly sensitive variable (Demoulin *et al*., 2012b).

However, a most interesting result of the model fitting comes from a comparison with independently derived values of m/n.

Meaning of the fitted m/n ratio

Although in the range of published values, the obtained m/n = 0.75 is significantly higher than the usual value around 0.5. One reason for this could be the presence of several strongly delayed knickpoints in the data set, an anomaly we have explained by their passing an erosion threshold. Indeed, this biases the best fit (m, K) couple towards a higher m value. We therefore fitted the stream power model to a smaller data set, from which the six most delayed knickpoints had been removed (Figure 9(D) shows that this leaves a much more homogeneous set of knickpoints). The recalculated best fit m (or m/n) value of 0.68 shows that, though lower, it still remains significantly different from 0.5. We now explore the implications of this, and begin with a comparison with independent estimates of m/n.

Based on field data collected in 38 rivers of the Ardennes (from which many sampled sites however display present alluvial conditions), Petit *et al*. (2005) estimated the value of the *b* and *c* exponents of Equations (3) and (4), linking channel width, discharge and drainage area, respectively to 0.49 (consistent with other studies, see Knighton (1998) and Wohl and David (2008))

and 0.98. From this and Equation (2), one derives a value of m/n = 0.50 for the currently graded reaches of the Ardennian rivers where the measurements were performed. A comparison of the relation between channel gradient and drainage area at steady state in detachment-limited conditions

$$S = \left(U \ K^{-1}\right)^{\frac{1}{n}} A^{\frac{-m}{n}} \tag{11}$$

where U is uplift, with the relation

$$S = k \ A^{-\theta} \tag{12}$$

that describes the log A–log S plots of river long profiles further shows that the latter's concavity θ is equivalent to m/n, thus providing another way to obtain this ratio from graded long profiles. Based on the five main rivers of the Ourthe catchment, and assuming that actual profile concavity is an acceptable approximation for intrinsic concavity (Whipple and Tucker, 2002), the mean concavity estimated from the part of their long profiles situated downstream of their respective knickpoint amounts to 0·55, a figure close to that derived from field measurements of Q_b and w_b. These values around 0·5, representative of the part of the Ourthe catchment presently at equilibrium, are significantly different from 0.68, the value derived from the knickpoint analysis.

Coming back to Equation (2), it seems improbable that *c*, the exponent of the power function linking discharge to drainage area, have much changed over time since the post-YMT incision started in NE Ardennes. Consequently, the difference in m/n value should mainly come from a difference in *b*, the exponent determining channel width as a function of discharge. In this reasoning, the m/n value of 0.68 yielded by the model fit should correspond to a *b* value around 0·32, remarkably similar to the average $b = 0·35$ compiled by Lague (2014) from published data for steady state incising bedrock rivers. Deduced from the knickpoint analysis, this value thus refers especially to channel width at the passage of the knickpoint, i.e. to the channel narrowing traveling in concert with the tip of the erosion wave.

Finnegan *et al*. (2005) and Whittaker *et al*. (2007a) have shown that channel width behavior during transient states is not described adequately if taken only as a power function of discharge, and that a dynamic dependence on channel gradient, which they derived either from the Manning equation (Finnegan *et al*., 2005) or from field data (Whittaker *et al*., 2007a), has also to be included. Indeed, in the transient case, the reach of steepened gradient propagated by the erosion wave carries a component of flow velocity-dependent channel narrowing decoupled from local discharge that has also to be accounted for. However, as the n = 1 assumption results in a knickpoint celerity modeling that does not involve local channel gradient, and in the advection of a constant-gradient knickpoint, the S^{-d} factor appearing in the Finnegan *et al*. (2005) expression of channel width, linked solely to the knickpoint's constant gradient, is also constant. It is therefore incorporated de facto in the coefficient of the functional relation between *w* and *Q*, thus also in the K coefficient of the incision model equation.

Erosivity coefficient

As for the second parameter yielded by the model fit, the coefficient of erosivity K, beyond the effects of uncertainty on the age of the erosion wave and of spatially variable controls, discussed above, we only want to stress that it was determined under the assumption of continuous incision since 700 ka. Yet, all models of Quaternary river incision in NW Europe (and in many places elsewhere) agree that only a limited part of the

glacial–interglacial cycle provides a balance between sediment load and efficient discharge that is favorable to incision (Vandenberghe, 1995, 2003, 2008; Bridgland, 2000; Bridgland and Westaway, 2008; Gibbard and Lewin, 2009; Lewin and Gibbard, 2010), which means that actual erosivity K and erosion rate *E* should be higher than their modeled values. Obviously, this part of the cycle allowing incision depends also on local conditions of, e.g., channel gradient and sediment flux, and it lasted thus probably longer at the beginning of the process, when knickpoints were forming in response to active uplift, than in recent times, when the drainage system response approached completion near the headwaters. Based on the many observations of floodplain aggradation during the main part of glacials and limited changes during interglacials, we may reasonably estimate that, all in all, fluvial incision actually took place during a maximum 20–30% of the total time elapsed since post-YMT erosion started. As K varies in strict inverse proportion with time in the incision equation, our best fit K should therefore probably be multiplied by a factor 3 to 5.

Conclusions

We analyzed a set of knickpoints associated with the post-YMT erosion wave that migrates in the Ourthe catchment of NE Ardennes since 0.7 Ma, and showed that the use of the simplest form of the knickpoint celerity equation derived from the stream power model of bedrock channel incision allowed a fairly good fit (based on time residual minimization) to the data that yielded a m/n value of 0.75. The analysis of the time residuals of the adjustment showed that they do not depend on rock resistance to erosion. Their variance is chiefly explained by the length of the trajectory followed by each knickpoint, the highest delays being observed in small tributaries of the lower half of the catchment. Most of these small tributaries display all features characteristic of hanging valleys. Knickpoint delays in fact correlate inversely with the time when the migrating erosion wave entered very small streams where it encountered an erosion threshold that more or less stopped its progression. Removing the knickpoints stopped at such thresholds from the data set, we calculated an improved m/n = 0.68. However, this value still contrasts with independent estimates around 0.50–0.55 obtained for the same ratio either from field data or long profiles of the currently graded downstream part of the catchment's streams. This discrepancy seems to arise mainly from the gradient-dependent bedrock channel narrowing (with respect to steady state channel width) accompanying the migrating knickpoint, which translates into a decreased exponent in the expression of channel width as a power function of discharge. Further research should now focus on the controls of the erosion threshold generally located just past the junction towards small tributaries, abrupt changes in the ratio between bed load grain size and river competence being a possible explicative factor. This is fundamental, because of the potential impact on the response time of the landscape as a whole to tectonic uplift.

References

Alexandre J. 1957. Les terrasses des bassins supérieurs de l'Ourthe et de la Lesse. *Annales de la Société Géologique de Belgique* **80**: 317–332.

Amos C, Burbank D. 2007. Channel width response to differential uplift. *Journal of Geophysical Research* **112**: F02010. DOI:10.1029/2006JF000672.

Anderson R, Anderson S. 2010. *Geomorphology. The Mechanics and Chemistry of Landscapes.* Cambridge University Press.

Anthony D, Granger D. 2007. An empirical stream power formulation for knickpoint retreat in Appalachian Plateau fluviokarst. *Journal of Hydrology* **343**: 117–126.

Antoine P, Lautridou JP, Laurent M. 2000. Long-term fluvial archives in NW France: response of the Seine and Somme rivers to tectonic movements, climatic variations and sea-level changes. *Geomorphology* **33**: 183–207.

Attal M, Cowie P, Whittaker A, Hobley D, Tucker G, Roberts G. 2011. Testing fluvial erosion models using the transient response of bedrock rivers to tectonic forcing in the Apennines, Italy. *Journal of Geophysical Research* **116**: F02005. DOI:10.1029/2010JF001875.

Attal M, Tucker G, Whittaker A, Cowie P, Roberts G. 2008. Modeling fluvial incision and transient landscape evolution: Influence of dynamic channel adjustment. *Journal of Geophysical Research* **113**: F03013. DOI:10.1029/2007JF000893.

Berlin M, Anderson R. 2007. Modeling of knickpoint retreat on the Roan Plateau, western Colorado. *Journal of Geophysical Research* **112**: F03S06. DOI:10.1029/2006JF000553.

Bishop P, Hoey T, Jansen J, Artza I. 2005. Knickpoint recession rate and catchment area: the case of uplifted rivers in Eastern Scotland. *Earth Surface Processes and Landforms* **30**: 767–778.

Boenigk W, Frechen M. 2006. The Pliocene and Quaternary fluvial archives of the Rhine system. *Quaternary Science Reviews* **25**: 550–574.

Bridgland D. 2000. River terrace systems in north-west Europe: an archive of environmental change, uplift, and early human occupation. *Quaternary Science Reviews* **19**: 1293–1303.

Bridgland D, Westaway R. 2008. Climatically controlled river terrace staircases: a worldwide Quaternary phenomenon. *Geomorphology* **98**: 285–315.

Brummer C, Montgomery D. 2003. Downstream coarsening in headwater channels. *Water Resources Research* **39**(10): 1294. DOI:10.1029/2003WR001981.

Camelbeeck T, Meghraoui M. 1998. Geological and geophysical evidence for large palaeoearthquakes with surface faulting in the Roer graben (northwestern Europe). *Geophysical Journal International* **132**: 347–362.

Castillo M, Bishop P, Jansen J. 2013. Knickpoint retreat and transient bedrock channel morphology triggered by base-level fall in small bedrock river catchments: The case of the Isle of Jura, Scotland. *Geomorphology* **180-181**: 1–9.

Cook K, Whipple K, Heimsath A, Hanks T. 2009. Rapid incision of the Colorado River in Glen Canyon - insights from channel profiles, local incision rates, and modeling of lithologic controls. *Earth Surface Processes and Landforms* **34**: 994–1010.

Cordier S, Harmand D, Frechen M, Beiner M. 2006. Fluvial system response to Middle and Upper Pleistocene climate change in the Meurthe and Moselle valleys (Paris basin and Rhenish Massif). *Quaternary Science Reviews* **25**: 1460–1474.

Cornet Y. 1995. L'encaissement des rivières ardennaises au cours du Quaternaire. In *L'Ardenne. Essai de géographie physique*, Demoulin A (ed.). Dépt Géographie Physique, Université de Liege: Liege; 155–177.

Cowie P, Whittaker A, Attal M, Roberts G, Tucker G, Ganas A. 2008. New constraints on sediment-flux-dependent river incision: Implications for extracting tectonic signals from river profiles. *Geology* **36**: 535–538.

Crosby B, Whipple K. 2006. Knickpoint initiation and distribution within fluvial networks: 236 waterfalls in the Waipaoa River, North Island, New Zealand. *Geomorphology* **82**: 16–38.

Crosby B, Whipple K, Gasparini N, Wobus C. 2007. Formation of fluvial hanging valleys: Theory and simulation. *Journal of Geophysical Research* **112**: F03S10. DOI:10.1029/2006JF000566.

Dehnert A, Kracht O, Preusser F, Akçar N, Kemna HA, Kubik P, Schlüchter C. 2011. Cosmogenic isotope burial dating of fluvial sediments from the Lower Rhine Embayment, Germany. *Quaternary Geochronology* **6**: 313–325.

Demoulin A, Beckers A, Bovy B. 2012b. On different types of adjustment usable to calculate the parameters of the stream power law. *Geomorphology* **138**: 203–208.

Demoulin A, Beckers A, Rixhon G, Braucher R, Bourlès D, Siame L. 2012a. Valley downcutting in the Ardennes (W Europe): Interplay between tectonically triggered regressive erosion and climatic cyclicity. *Netherlands Journal of Geosciences* **91**: 79–90.

Demoulin A, Hallot E. 2009. Shape and amount of the Quaternary uplift of the western Rhenish shield and the Ardennes (western Europe). *Tectonophysics* **474**: 696–708.

Demoulin A, Hallot E, Rixhon G. 2009. Amount and controls of the Quaternary denudation in the Ardennes massif (western Europe). *Earth Surface Processes and Landforms* **34**: 1487–1496.

Duvall A, Kirby E, Burbank D. 2004. Tectonic and lithologic controls on bedrock channel profiles and processes in coastal California. *Journal of Geophysical Research* **109**: F03002. DOI:10.1029/2003JF000086.

Ek C. 1957. Les terrasses de l'Ourthe et de l'Amblève inférieures. *Annales de la Société Géologique de Belgique* **80**: 333–353.

Finnegan N, Roe G, Montgomery D, Hallet B. 2005. Controls on the channel width of rivers: Implications for modeling fluvial incision of bedrock. *Geology* **33**: 229–232.

Finnegan N, Sklar L, Fuller T. 2007. Interplay of sediment supply, river incision, and channel morphology revealed by the transient evolution of an experimental bedrock channel. *Journal of Geophysical Research* **112**: F03S11. DOI:10.1029/2006JF000569.

Gasparini N, Bras R, Whipple K. 2006. Numerical modeling of non-steady-state river profile evolution using a sediment-flux-dependent incision model. In *Tectonics, Climate, and Landscape Evolution*, Willett S, Hovius N, Brandon M, Fisher D (eds). Geological Society of America Special Paper **398**; 127–141.

Gasparini N, Whipple K, Bras R. 2007. Predictions of steady state and transient landscape morphology using sediment-flux-dependent river incision models. *Journal of Geophysical Research* **112**: F03S09. DOI:10.1029/2006JF000567.

Gibbard P, Lewin J. 2009. River incision and terrace formation in the Late Cenozoic of Europe. *Tectonophysics* **474**: 41–55.

Hayakawa Y, Matsukura Y. 2009. Factors influencing the recession rate of Niagara Falls since the 19th century. *Geomorphology* **110**: 212–216.

Hoffmann R. 1996. Die quartäre Tektonik des südwestlichen Schiefergebirges begründet mit der Höhenlage der jüngeren Hauptterrasse der Mosel und ihrer Nebenflüsse. *Bonner Geowissenschaftliche Schriften* **19**.

Houtgast R, Van Balen R, Kasse C. 2005. Late Quaternary evolution of the Feldbiss Fault (Roer Valley Rift System, the Netherlands) based on trenching and its potential relation to glacial unloading. *Quaternary Science Reviews* **24**: 491–510.

Howard A, Dietrich W, Seidl M. 1994. Modeling fluvial erosion on regional to continental scales. *Journal of Geophysical Research* **99B**: 13971–13986.

Howard A, Kerby G. 1983. Channel changes in badlands. *Geological Society of America Bulletin* **94**: 739–752.

Jansen J, Fabel D, Bishop P, Xu S, Schnabel C, Codilean A. 2011. Does decreasing paraglacial sediment supply slow knickpoint retreat? *Geology* **39**: 543–546.

Juvigné E, Renard F. 1992. Les terrasses de la Meuse de Liège à Maastricht. *Annales de la Société Géologique de Belgique* **115**: 167–186.

Knighton D. 1998. *Fluvial forms and processes. A new perspective*. Arnold: London, 383 p.

Lague D. 2010. Reduction of long-term bedrock incision efficiency by short-term alluvial cover intermittency. *Journal of Geophysical Research* **115**: F02011. DOI:10.1029/2008JF001210.

Lague D. 2014. The stream power river incision model: evidence, theory and beyond. *Earth Surface Processes and Landforms* **39**: 38–61.

Lague D, Hovius N, Davy P. 2005. Discharge, discharge variability, and the bedrock channel profile. *Journal of Geophysical Research* **110**: F04006. DOI:10.1029/2004JF000259.

Lewin J, Gibbard P. 2010. Quaternary river terraces in England: Forms, sediments and processes. *Geomorphology* **120**: 293–311.

Loget N, Van Den Driessche J. 2009. Wave train model for knickpoint migration. *Geomorphology* **106**: 376–382.

Meyer W, Stets J. 1998. Junge Tektonik im Rheinischen Schiefergebirge und ihre Quantifizierung. *Zeitschrift der Deutschen Geologischen Gesellschaft* **149**: 359–379.

Meyer W, Stets J. 2007. Quaternary uplift in the Eifel area. In *Mantle plumes, A multidisciplinary approach*, Ritter J, Christensen U (eds). Springer; 369–378.

Montgomery D, Foufoula-Georgiou E. 1993. Channel network representation using digital elevation models. *Water Resources Research* **29**: 1178–1191.

Niemann J, Gasparini N, Tucker G, Bras R. 2001. A quantitative evaluation of Playfair's law and its use in testing long-term stream erosion models. *Earth Surface Processes and Landforms* **26**: 1317–1332.

Pelletier J. 2007. Numerical modeling of the Cenozoic geomorphic evolution of the southern Sierra Nevada, California. *Earth and Planetary Science Letters* **259**: 85–96.

Petit F, Hallot E, Houbrechts G, Mols J. 2005. Evaluation des puissances spécifiques de rivières de Moyenne et de Haute Belgique. *Bulletin de la Société Géographique de Liege* **46**: 37–50.

Pissart A. 1974. La Meuse en France et en Belgique. Formation du bassin hydrographique. Les terrasses et leurs enseignements. *Centenaire de la Société géologique de Belgique, L'évolution quaternaire des bassins fluviaux de la Mer du Nord méridionale*, Liege, 105–131.

Pissart A, Harmand D, Krook L. 1997. L'évolution de la Meuse de Toul à Maastricht depuis le Miocène: corrélations chronologiques et traces des captures de la Meuse lorraine d'après les minéraux denses. *Géographie Physique et Quaternaire* **51**: 267–284.

Quinif Y. 1999. Karst et évolution des rivières: le cas de l'Ardennes. *Geodinamica Acta* **12**, 267–277.

Ritter J, Jordan M, Christensen U, Achauer U. 2001. A mantle plume below the Eifel volcanic fields, Germany. *Earth and Planetary Science Letters* **186**: 7–14.

Rixhon G, Braucher R, Bourlès D, Siame L, Bovy B, Demoulin A. 2011. Quaternary river incision in NE Ardennes (Belgium) - Insights from [10]Be/[26]Al dating of river terraces. *Quaternary Geochronology* **6**: 273-284.

Roberts G, White N. 2010. Estimating uplift rate histories from river profiles using African examples. *Journal of Geophysical Research* **115**: B02406. DOI:10.1029/2009JB006692.

Roe G, Montgomery D, Hallet B. 2002. Effects of orographic precipitation variations on the concavity of steady-state river profiles. *Geology* **30**: 143–146.

Seidl A, Dietrich W. 1992. The problem of channel erosion into bedrock. *Catena Supplement* **23**: 101–124.

Selby M, 1980. A rock mass strength classification for geomorphic purposes, with tests from Antarctica and New Zealand. *Zeitschrift für Geomorphologie* **24**: 31–51.

Sklar L, Dietrich W. 1998. River longitudinal profiles and bedrock incision models: Stream power and the influence of sediment supply. In *Rivers Over Rock: Fluvial Processes in Bedrock Channels*, Tinkler K, Wohl E (eds). Geophysical Monographies Series, 107, AGU: Washington DC; 237–260.

Sklar L, Dietrich W. 2001. Sediment and rock strength controls on river incision into bedrock. *Geology* **29**: 1087–1090.

Sklar L, Dietrich W. 2004. A mechanistic model for river incision into bedrock by saltating bed load. *Water Resources Research* **40**: W06301. DOI:10.1029/2003WR002496.

Sklar L, Dietrich W. 2006. The role of sediment in controlling steady-state bedrock channel slope: Implications of the saltation-abrasion incision model. *Geomorphology* **82**: 58–83.

Snyder N, Kammer L. 2008. Dynamic adjustments in channel width in response to a forced diversion: Gower Gulch, Death Valley National Park, California. *Geology* **36**: 187–190.

Snyder N, Whipple K, Tucker G, Merritts D. 2000. Landscape response to tectonic forcing: Digital elevation model analysis of stream profiles in the Mendocino triple junction region, northern California. *Geological Society of America Bulletin* **112**: 1250–1263.

Stark C. 2006. A self-regulating model of bedrock river channel geometry. *Geophysical Research Letters* **33**: L04402. DOI:10.1029/2005GL023193.

Stock J, Montgomery D. 1999. Geologic constraints on bedrock river incision using the stream power law. *Journal of Geophysical Research* **104B**: 4983–4993.

Tinkler K, Wohl E (eds). 1998. Rivers over Rock: Fluvial Processes in Bedrock Channels. *Geophysical Monograph Series 107*, American Geophysical Union: Washington, D. C.

Tucker G, Slingerland R. 1997. Drainage basin responses to climate change. *Water Resources Research* **33**: 2031–2047.

Turowski J, Hovius N, Meng-Long H, Lague D, Men-Chiang C. 2008. Distribution of erosion across bedrock channels. *Earth Surface Processes and Landforms* **33**: 353–363.

Turowski J, Lague D, Hovius N. 2007. Cover effect in bedrock abrasion: a new derivation and its implications for the modeling of bedrock channel morphology. *Journal of Geophysical Research* **112**: F04006. DOI:10.1029/2006JF000697.

Valla P, van der Beek P, Lague D. 2010. Fluvial incision into bedrock: Insights from morphometric analysis and numerical modeling of gorges incising glacial hanging valleys (Western Alps, France). *Journal of Geophysical Research* **115**: F02010. DOI: 10.1029/2008JF001079.

Van Balen R, Houtgast R, Van der Wateren F, Vandenberghe J, Bogaart P. 2000. Sediment budget and tectonic evolution of the Meuse catchment in the Ardenness and the Roer Valley Rift System. *Global and Planetary Change* **27**: 113–129.

Van den Berg M. 1996. *Fluvial sequences of the Maas. A 10 Ma record of neotectonics and climate change at various time-scales.* Landbouwuniversiteit: Wageningen.

Van der Beek P, Bishop P. 2003. Cenozoic river profile development in the Upper Lachlan catchment (SE Australia) as a test of quantitative fluvial incision models. *Journal of Geophysical Research* **108B**: 2309. DOI:10.1029/2002JB002125.

Vandenberghe J. 1995. Timescales, climate and river development. *Quaternary Science Reviews* **14**: 631–638.

Vandenberghe J. 2003. Climate forcing of fluvial system development: an evolution of ideas. *Quaternary Science Reviews* **22**: 2053–2060.

Vandenberghe J. 2008. The fluvial cycle at cold–warm–cold transitions in lowland regions: A refinement of theory. *Geomorphology* **98**: 275–284.

Vandenberghe J, Kasse C, Bohncke S, Kozarski S. 1994. Climate-related river activity at the Weichselian–Holocene transition: a comparative study of the Warta and Maas rivers. *Terra Nova* **6**: 476–485.

Whipple K, Hancock G, Anderson R. 2000. River incision into bedrock: Mechanics and relative efficacy of plucking, abrasion and cavitation. *Geological Society of America Bulletin* **112**: 490–503.

Whipple K, Tucker G. 1999. Dynamics of the stream-power river incision model: implications for height limits of mountain ranges, landscape response timescales, and research needs. *Journal of Geophysical Research* **104B**: 17661–17674.

Whipple K, Tucker G. 2002. Implications of sediment-flux-dependent river incision models for landscape evolution. *Journal of Geophysical Research* **107B**: 2039. DOI:10.1029/2000JB000044.

Whitbread K. 2012. Postglacial evolution of bedrock rivers in post-orogenic terrains: the NW Scottish Highlands. Unpublished PhD thesis, University of Glasgow. Available at: http://theses.gla.ac.uk/3499/.

Whittaker A, Attal M, Cowie P, Tucker G, Roberts G. 2008. Decoding temporal and spatial patterns of fault uplift using transient river long profiles. *Geomorphology* **100**: 506–526.

Whittaker A, Boulton S. 2012. Tectonic and climatic controls on knickpoint retreat rates and landscape response times. *Journal of Geophysical Research* **117**: F02024. DOI:10.1029/2011JF002157.

Whittaker A, Cowie P, Attal M, Tucker G, Roberts G. 2007a. Bedrock channel adjustment to tectonic forcing: Implications for predicting river incision rates. *Geology* **35**: 103–106.

Whittaker A, Cowie P, Attal M, Tucker G, Roberts G. 2007b. Contrasting transient and steady-state rivers crossing active normal faults: New field observations from the central Apennines, Italy. *Basin Research* **19**: 529–556.

Willgoose G, Bras R, Rodriguez-Iturbe I. 1991. A coupled channel network growth and hillslope evolution model. 1. Theory. *Water Resources Research* **27**: 1671–1684.

Wobus C, Crosby B, Whipple K. 2006. Hanging valleys in fluvial systems: Controls on occurrence and implications for landscape evolution. *Journal of Geophysical Research* **111**: F02017. DOI:10.1029/2005JF000406.

Wohl E, David G. 2008. Consistency of scaling relations among bedrock and alluvial channels. *Journal of Geophysical Research* **113**: F04013. DOI:10.1029/2008JF000989.

Yanites B, Tucker G, Mueller K, Chen Y, Wilcox T, Huang S, Shi K. 2010. Incision and channel morphology across active structures along the Peikang River, central Taiwan: Implications for the importance of channel width. *Geological Society of America Bulletin* **122**: 1192–1208.

Zhang H, Zhang P, Fan Q. 2011. Initiation and recession of the fluvial knickpoints: A case study from the Yalu River – Wangtian'e volcanic region, northeastern China. *Science China Earth Science* **54**: 1746–1753. DOI: 10.1007/s11430-011-4254-6.

Ziegler P, Dèzes P. 2007. Cenozoic uplift of Variscan massifs in the Alpine foreland: Timing and controlling mechanisms. *Global and Planetary Change* **58**: 237–269.